microplastics

MDPI

Review

Microplastics Across the Human Body: Occurrence, Detection Methodologies, and Distribution in Human Tissues, Organs, and Biological Fluids

Hriddhi Sarker [1], Umar Hasnain Monabbi [1], Goutam Saha [2,*], Awnon Bhowmik [3] and B. M. Rabby Hossain [4]

[1] Department of Biochemistry and Molecular Biology, University of Rajshahi, Rajshahi 6205, Bangladesh; hriddhisarkerborno@gmail.com (H.S.); hasnainumar2001@gmail.com (U.H.M.)
[2] Department of Mathematics, International University of Business Agriculture and Technology, Dhaka 1230, Bangladesh
[3] College of Engineering & Computer Science, Colorado Technical University, Colorado Springs, CO 80907, USA; awnonbhowmik@outlook.com
[4] Department of Disaster Science and Climate Resilience, University of Dhaka, Dhaka 1000, Bangladesh; hossain.dsm@du.ac.bd
* Correspondence: gsahamath@du.ac.bd

Abstract

The rapid growth in plastic production and consumption has led to the widespread contamination of the environment with microplastics (MPs), raising increasing concerns about their potential impacts on human health. In recent years, advances in analytical techniques have revealed the presence of MPs in a wide range of human biological samples, suggesting that these particles can enter, circulate within, and accumulate throughout the human body. This narrative review provides a comprehensive overview of the current evidence on the occurrence and distribution of MPs in human tissues, organs, and biological fluids. MPs have been detected in blood, urine, stool, semen, breast milk, amniotic fluid, ocular fluids, and lavage fluids, as well as in several organs and tissues including the lungs, placenta, heart, kidneys, liver, vascular tissues, and reproductive organs. Among the identified polymers, polyethylene (PE), polypropylene (PP), polyethylene terephthalate (PET), polystyrene (PS), and polyvinyl chloride (PVC) are reported most frequently. This narrative review also summarizes the major analytical techniques used for MP detection and characterization, including Raman spectroscopy, μ-FTIR, LDIR spectroscopy, and Py-GC/MS, which highlight their advantages and limitations. Collectively, the available evidence demonstrates that MPs are not confined to the external environment but are now detectable in multiple compartments of the human body, including highly protected biological systems. However, important questions remain regarding their long-term persistence, transport mechanisms, biological fate, and potential health effects. Further methodological standardization and large-scale human studies are needed to better understand the extent of human exposure and the implications of MP accumulation for human health.

Keywords: microplastics; human body; biological fluids; tissues; organs

Check for updates

Academic Editors: Jose Manuel Cervantes-Uc and Nicolas Kalogerakis

Received: 7 June 2026
Revised: 11 July 2026
Accepted: 5 August 2026
Published: 7 August 2026

Copyright: © 2026 by the authors. Licensee MDPI, Basel, Switzerland. This article is an open access article distributed under the terms and conditions of the Creative Commons Attribution (CC BY) license.

1. Introduction

Microplastics (MPs) are plastic particles smaller than 5 mm in size and have emerged as a growing environmental and public health concern worldwide [1]. The term "Microplastics" was first introduced by Professor Richard Thompson in 2004 to describe small plastic fragments detected in marine environments [2]. Based on their origin, MPs are generally

classified into primary and secondary MPs. Primary MPs are intentionally manufactured at microscopic sizes and are released into the environment through products such as cosmetics, personal care items, industrial abrasives, and synthetic textiles. In contrast, secondary MPs originate from the fragmentation and degradation of larger plastic materials through physical, chemical, and biological processes, including ultraviolet radiation, weathering, and mechanical abrasion [3]. Recent evidence further suggests that, beyond environmental weathering and mechanical abrasion, residual stresses generated during plastic manufacturing can induce phase separation within polymers, promoting the release of amorphous polymer micropollutants and broadening the current understanding of plastic pollutant generation [4]. Owing to the extensive production and widespread use of plastic materials in modern society, MPs have become ubiquitous contaminants that are now detected in air, water, soil, food products, and numerous ecological systems. Consequently, human exposure to MPs occurs through multiple pathways, including inhalation, ingestion, and dermal contact, raising increasing concerns regarding their potential accumulation in the human body and associated health risks [5].

The global production of plastics has risen markedly over recent decades, reaching an estimated 430.9 million metric tons in 2024. China accounts for the largest proportion of this production, followed by other Asian countries and North America [6]. Although plastics provide substantial societal and economic benefits, the rapid increase in their production and consumption has accelerated the accumulation of plastic waste, leading to the pervasive presence of MPs in environmental compartments and, increasingly, in human tissues and biological fluids.

In recent years, increasing numbers of studies have reported the presence of MPs in human blood, placenta, lungs, reproductive tissues, urine, stool, and many other biological samples [7–15]. These findings have raised growing concerns about the extent of human exposure and the possible consequences for human health [16,17]. However, the available evidence remains scattered across different research fields. Most studies focus on specific organs, tissues, or body fluids, making it difficult to obtain a complete picture of how MPs are distributed throughout the human body [18–20]. In addition, researchers have used a wide variety of approaches to isolate, identify, and quantify MPs. Differences in sample digestion procedures, filtration methods, particle recovery strategies, and analytical techniques can greatly influence the reported results. Consequently, findings often vary between studies, and direct comparisons are not always straightforward. While advanced technologies such as Raman spectroscopy, μ-FTIR, LDIR spectroscopy, and Py-GC/MS have become widely used in human MP research, their respective strengths, limitations, and suitability for different biological samples have not been discussed together in a comprehensive and accessible manner. At the same time, evidence of MP accumulation in multiple human tissues and body fluids continues to grow. Reports have identified MPs in highly protected biological environments, including the placenta, reproductive tissues, blood circulation, and internal organs, suggesting that these particles may move throughout the body and reach sites previously considered less vulnerable to environmental contaminants [21,22]. Despite these important findings, information regarding their distribution patterns, bioaccumulation, and potential health implications remains dispersed across numerous studies, making it challenging for researchers, clinicians, and policymakers to fully understand the broader picture.

In addition to their origin-based classification, plastic particles are also distinguished by size. Nanoplastics (NPs) are generally defined as plastic particles smaller than 1 μm, whereas MPs smaller than 10 μm are increasingly recognized as a major analytical challenge in human biomonitoring because they are difficult to recover during sample preparation and frequently fall below the practical detection limits of conventional analytical techniques

such as μ-FTIR, Raman spectroscopy, and LDIR. Although Raman spectroscopy provides higher spatial resolution than μ-FTIR and LDIR, the reliable identification and quantification of ultrafine plastic particles remain constrained by limited analytical sensitivity and the lack of standardized analytical protocols. Due to their much smaller size, NPs exhibit physicochemical properties and biological behaviors distinct from those of larger MPs, including enhanced cellular uptake, intracellular transport, and an increased ability to cross biological barriers such as the intestinal epithelium, placenta, and blood–brain barrier [23]. Consequently, most human biomonitoring studies predominantly report MPs, whereas many mechanistic and toxicological studies employ engineered NPs to investigate cellular uptake and biological effects under controlled experimental conditions, reflecting the current technical limitations in detecting environmentally relevant NPs in human biological samples [24].

Therefore, this narrative review brings together current evidence on the detection of MPs in human biological samples. It systematically examines sample preparation strategies and analytical methodologies, compares the major techniques used for MP identification, and synthesizes the available evidence on their occurrence and distribution across human tissues, organs, and biological fluids. By integrating findings from these diverse areas, this review identifies methodological challenges, summarizes current knowledge gaps, and outlines priorities for future research. Figure 1 illustrates the overall pathway from global plastic production and environmental pollution to human exposure, tissue accumulation, and the potential biological effects of MPs.

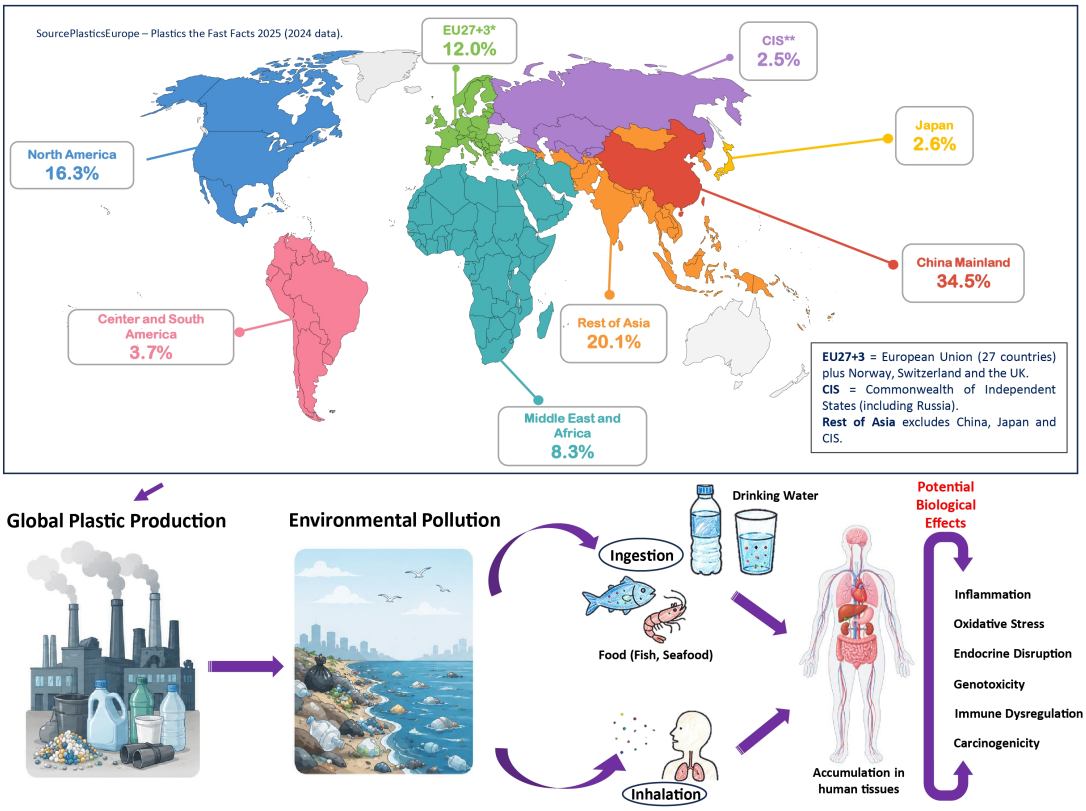


Figure 1. Schematic overview of the progression from global plastic production and environmental pollution to human exposure pathways, tissue accumulation, and the potential biological effects of microplastics in the human body. (* European Union (27 countries) plus Norway, Switzerland and the UK and ** Commonwealth of Independent States (including Russia).

2. Literature Search and Study Selection

The literature search is conducted using two major academic databases: Scopus and Google Scholar. These databases are selected to ensure a broad, multidisciplinary capture of both peer-reviewed articles. The search is restricted to articles published between January 2021 and April 2026. A combination of Medical Subject Headings and free-text terms is used. The core search string applied was: ("microplastic" OR "microplastics" OR "nanoplastic" OR "nanoplastics") AND ("human" OR "human body" OR "human tissue" OR "human organ" OR "biological fluid" OR "blood" OR "urine" OR "semen" OR "breast milk" OR "amniotic fluid" OR placenta* OR "lung* OR "liver" OR "kidney" OR "heart"). We have considered the following inclusion criteria: i. Original research articles (e.g., observational, cross-sectional, case studies) published in English; ii. Studies that detected and characterized MPs in actual human tissues, organs, or biological fluids; iii. Studies utilizing validated spectroscopic (Raman, FTIR, LDIR) or thermo-analytical (Py-GC/MS) techniques for polymer identification. We have also considered the following exclusion criteria: i. In vitro or animal model studies. ii. Review articles, conference abstracts, book chapters, and editorials. iii. Studies focusing exclusively on environmental, food, or water matrices without direct human sampling. Since this is a narrative review aimed at synthesizing methodologies and distribution patterns rather than performing a meta-analysis, a formal PRISMA flow diagram is not utilized. However, to ensure reproducibility and mitigate selection bias, we have provided a detailed textual description of the screening process. Initially, duplicate records between Scopus and Google Scholar are removed. Subsequently, titles and abstracts are screened against the inclusion/exclusion criteria. Full-text articles of potentially relevant studies are then retrieved and assessed for eligibility. Discrepancies regarding inclusion are resolved through discussion among the authors until a consensus is reached.

3. Methodological Approaches for MP Detection

The detection and characterization of MPs in human biological samples involve multiple methodological steps, including sample preparation, particle isolation, and analytical identification. Because human tissues and body fluids contain complex organic matrices, efficient digestion and filtration procedures are essential to isolate MPs prior to analysis. In recent years, various spectroscopic and thermo-analytical techniques have been increasingly applied for polymer identification and quantification.

3.1. Sample Preparation and Filtration

Sample preparation and filtration represent critical initial steps in MP analysis, as they directly affect particle recovery and downstream identification. The primary objective of sample preparation is to remove organic matter while preserving the integrity of MPs. Following digestion, filtration and particle isolation are performed to recover particles of different size ranges for subsequent spectroscopic or chemical characterization. Different studies have employed diverse digestion reagents, filtration materials, and pore sizes depending on the biological matrix and analytical technique used, contributing to significant methodological heterogeneity across the literature.

3.1.1. Sample Digestion Methods

To study MPs in human samples, biological materials must first undergo digestion to remove organic tissues and cells while leaving the plastic particles intact. As shown in Table 1, studies employed a wide range of digestion methods, with the choice depending primarily on sample type (fluid vs. solid tissue) and the downstream analytical technique.

Among the most widely applied approaches, alkaline digestion using potassium hydroxide (KOH) was the most common, typically at concentrations of 10–30% under controlled temperature and time conditions. For instance, several studies used 10% KOH at 40–60 °C for 24–72 h to effectively dissolve organic matter while preserving MPs [15,25–28]. In some cases, prolonged digestion durations (up to 7–14 days at room temperature) were employed to ensure complete tissue degradation, especially for complex matrices such as placenta or tumor tissues [12,29].

Oxidative digestion using hydrogen peroxide (H_2O_2) was another common method, often used alone or together with KOH. This approach was especially popular for blood, bronchoalveolar lavage fluid, and soft tissues. In this process, samples were usually incubated for several days, sometimes up to 11 days at temperatures between 55 °C and 65 °C. This gentle process slowly breaks down organic matter while helping to protect the MPs from damage [30–32]. Some studies have also applied a sequential two-step digestion method, in which samples are first treated with KOH followed by H_2O_2, to enhance the efficiency of organic matter removal [13,33].

Acid-based digestion, particularly using concentrated nitric acid (HNO_3), was another widely used method. This was especially common in studies that employed Py-GC/MS for polymer identification and quantification. These protocols typically involved incubation at room temperature for 48 h, followed by heating at 95–110 °C. While highly effective at removing organic matter, there is increasing concern that vigorous digestion with concentrated nitric acid may degrade certain susceptible polymers, particularly polyamide (PA/nylon), and alter the morphology or size of other polymers, potentially affecting their subsequent identification and quantification [34]. Therefore, the choice of digestion protocol should carefully balance efficient organic matter removal with preservation of polymer integrity [35–39].

Comparative evaluations of digestion protocols have demonstrated that the preservation of microplastic integrity depends not only on the digestion reagent but also on its concentration, temperature, and exposure duration. Alkaline digestion using KOH generally exhibits high compatibility with common polymers, including PE, PP, PS, and PET, while causing minimal changes in particle morphology and FTIR or Raman spectra under optimized conditions [40,41]. In comparison, hydrogen peroxide (H_2O_2) is considered one of the least aggressive chemical digestion agents and effectively removes organic matter with minimal alteration to the physicochemical properties of most polymers, although prolonged exposure or elevated temperatures may affect more susceptible materials [41,42]. Conversely, strong acid digestion using concentrated nitric acid (HNO_3), despite its high digestion efficiency, has been reported to induce oxidation, surface erosion, particle fragmentation, and spectral alterations in certain polymers, particularly polyamide (PA), polyurethane (PU), and, under harsh conditions, PET, thereby increasing the risk of polymer degradation and inaccurate identification. Overall, comparative evaluations suggest that no single digestion protocol is universally suitable for all biological matrices, and the optimal method should be selected by balancing digestion efficiency with preservation of particle morphology, polymer chemistry, and compatibility with subsequent analytical techniques such as μ-FTIR, Raman spectroscopy, and Py-GC/MS [40–42].

For more sensitive applications where preservation of small MPs and NPs is critical, enzymatic digestion methods were employed. These protocols typically used proteinase K combined with SDS, Tris-HCl, and $CaCl_2$ under mild conditions (e.g., 60 °C for 8 h followed by room temperature incubation). Although gentler on the particles, these methods usually require longer processing times and strictly controlled conditions [11,43,44].

In addition, some studies used combined or alternative strategies such as NaOH with H_2O_2, KOH-NaClO mixtures, or solvent extraction (e.g., chloroform, xylene, hexafluo-

roisopropanol). The choice depended on the sample type and the analytical technique to be used afterwards [45–47]. Some studies also incorporated mechanical pre-treatments such as freeze-drying (lyophilization), grinding, and sieving before chemical digestion [48]. Notably, a few researchers avoided the filtration step entirely to prevent losing very small particles (<10 µm), which highlights a key limitation of conventional methods [49].

Therefore, these findings indicate that KOH-based alkaline digestion remains the most commonly used and cost-effective method for extracting MPs from human samples. Nevertheless, no universally standardized protocol currently exists. The selection of digestion technique reflects a trade-off between efficient organic matter removal, preservation of MPs (particularly smaller particles and nanoplastics), and compatibility with downstream analytical techniques such as µ-FTIR, Raman spectroscopy, LDIR, or Py-GC/MS. This methodological heterogeneity likely contributes to the observed variability in MP detection and quantification across studies and highlights the urgent need for standardized protocols in future research.

3.1.2. Filtration and Particle Isolation

Following digestion, filtration and particle isolation are critical steps for the recovery and characterization of MPs from human samples. Across the narrative reviewed studies, a wide variety of filter materials and pore sizes were used, reflecting differences in analytical goals and target particle sizes.

The most commonly employed filters included glass fiber filters (e.g., Whatman GF/A, GF/C, GF/F with pore sizes 0.7–1.6 µm), silver membrane filters (0.45 µm), polytetrafluoroethylene (PTFE) membranes (0.2–1 µm), stainless steel meshes (10–13 µm), and aluminum oxide (Anodisc) filters (0.02 µm). Glass fiber filters were widely used across studies for MP recovery and subsequent analysis [15,29,30]. Silver membrane filters (0.45 µm) are frequently employed for the detection of smaller MPs and are commonly used in studies involving Raman and µ-FTIR spectroscopic analysis [13,25,27,33]. PTFE membranes (0.2–1 µm) were used in several studies for the isolation of fine MP particles [50,51]. For the detection of ultra-small particles, aluminum oxide (Anodisc) filters with 0.02 µm pore size were utilized [31,32,43].

In contrast, stainless steel meshes with larger pore sizes (10–13 µm) were used in some studies, particularly when focusing on larger MPs or when preventing clogging in dense or viscous samples [35–37,45]. However, these approaches may underestimate the smaller particle fractions. Mixed cellulose ester membranes (5 µm) and silica-based filters (1 µm) were also applied in specific contexts, balancing particle retention with analytical compatibility [52,53].

Vacuum-assisted filtration systems were commonly used across studies to facilitate particle recovery. In some studies, additional processing steps such as sample rinsing were incorporated to improve particle recovery [33,54,55]. In certain cases, staining techniques were applied to assist in the visualization of MP particles [14]. Notably, methodological variations also extended to particle isolation strategies. While most studies relied on direct filtration, a few adopted alternative particle isolation approaches that did not exclusively depend on conventional filtration methods. For example, Montano et al. [49] applied a modified extraction and analytical workflow for the detection of small particles. Thus, filtration and particle isolation methods exhibit considerable heterogeneity across studies. Capturing smaller particles requires the use of finer pore-size filters; however, this often slows the filtration process and increases the risk of clogging. As different studies employ varying filtration materials and pore sizes, the reported results can differ significantly, particularly in terms of MP abundance and size distribution. Therefore, this methodological

variability highlights the need for harmonized and standardized filtration protocols in future research to ensure comparability across studies.

3.1.3. Methodological Standardization and Harmonization

The studies summarized in Table 1 highlight substantial methodological heterogeneity in sample preparation and particle isolation workflows. Variations in digestion protocols, filtration materials and pore sizes, particle isolation strategies, and analytical workflows can influence MP recovery efficiency, detection limits, and the reported abundance, size distribution, and polymer composition across studies. Consequently, direct comparisons among studies remain challenging. Although methodological choices are often determined by the biological matrix and downstream analytical technique, the absence of standardized protocols remains a major limitation in current human biomonitoring research. Therefore, the development of harmonized methodologies for sample preparation, filtration, particle isolation, and analytical validation is essential to improve reproducibility and enable reliable cross-study comparisons.

Table 1. Sample preparation and filtration methods.

Ref.	Sample Preparation	Filtration
Xu et al. [25]	• Tissues: Digested using 10% KOH solution (50 °C, 48 h) followed by 30% H_2O_2 (25 °C, 24 h). • Blood: Denatured with Tris-HCl buffer/SDS (60 °C) and digested with Proteinase K (50 °C).	• Silver membrane filter (0.45 µm).
Wang et al. [26]	• Placenta: 10% Potassium Hydroxide (KOH) solution (1 g tissue per 30 mL) incubated at 50 °C with agitation (120 rpm) for 72 h.	• Stainless steel membranes (pore size 10 µm).
Özgen Alpaydin et al. [30]	• Body fluids (blood and BAL): Digested using 30% H_2O_2. Incubated in shaking incubator at 55 °C for approx. 11 days (or until no visible tissue remained) at 65 rpm. • Additional H_2O_2 added after 5 days.	• Glass microfiber filters (Whatman GF/F, Pore size: 0.7 µm)
Wang et al. [35]	• Py-GC/MS: Digested with conc. HNO_3 (65%) at RT for 48 h, then heated at 110 °C for 3 h. • LDIR (Bile): Enzymatic digestion (SDS, $CaCl_2$, Tris-HCl, enzymes) at 60 °C for 8 h. LDIR (Tissue): Digested with 68% Nitric Acid for 12 h.	-
Halfar et al. [56]	• Amniotic Fluid: Digested using 30% KOH solution (1:1 *v*/*v*) for 24 h at RT. • Placenta: Tissue samples (0.5 g) treated with 10% KOH solution at 37 °C for 2 h, followed by 22 h at RT.	• Glass fiber filters with a pore size of 1 µm.

Table 1. *Cont.*

Ref.	Sample Preparation	Filtration
Jenner et al. [31]	• Digested using 100 mL of 30% Hydrogen Peroxide. • Then placed in a shaking incubator at 55 °C for approximately 11 days (or until no visible tissue remained).	• Filtered onto aluminum oxide filters (pore size 0.02 µm, Anodisc).
Zhao et al. [12]	• LDIR: Digested using an enzyme liquid system (0.05% SDS, 5 mmol $CaCl_2$, 1 mol Tris-HCl, pH = 8) incubated at 60 °C for 8 h, then room temperature for 3 days. • Py-GC/MS: Digested with concentrated nitric acid (1:3 w/v) for 48 h at room temperature.	• Filtered through a 0.45 µm membrane.
Montano et al. [15]	• Digested using a 10% KOH solution (1:2 ratio v/v) for 48 h at 40 °C.	• Filtered through glass microfiber filters (Whatman GF/C) with a pore size of 1.2 µm.
Sun et al. [36]	• Digested using 68% concentrated nitric acid for 48 h at room temperature • Heated at 95 °C for at least 3 h.	• Filtered through a stainless steel membrane (pore size 13 µm).
Zong et al. [45]	• Treated with sodium hydroxide solution and 15 mL of 30% hydrogen peroxide for digestion at room temperature for 12 h.	• Filtered using a 13 µm stainless steel mesh.
Wang et al. [37]	• Digested with concentrated nitric acid (1:3 ratio v/v) for 48 h at room temperature. • Heated at 95 °C for at least 3 h.	• Filtered through a 13 µm stainless steel mesh.
Zhao et al. [12]	• Digested using a 10% KOH solution (1:6 ratio). • Stored at 20 °C for 14 days.	• Filtered through a 1.6 µm glass fiber filter.
Dong et al. [27]	• Digested using 10% KOH solution (1:1 v/v ratio) for 48 h at 40 °C in a shaker incubator.	• Filtered through a 0.45 µm silver filter membrane.
Montano et al. [49]	• A new patented method was used to extract MPs without a filtration step to prevent the loss of NPs and MPs < 10 µm.	-
Ragusa et al. [29]	• Digested using a 10% KOH solution at room temperature for 7 days.	• Filtered through 1.6 µm glass fiber filter paper (Whatman GF/A).

Table 1. *Cont.*

Ref.	Sample Preparation	Filtration
Massardo et al. [51]	• Dissolved in 200 mL (tissue) or 250–300 mL (urine) of a 10% KOH solution. • Sealed jars were placed in an incubator at 60 °C for 5 days until the solution became limpid.	• Vacuum-filtered using PTFE filter membranes with a 0.2 µm pore size.
Leonard et al. [43]	• Blood decanted into Durham bottle with tris buffer (pH 8), pig pancreatic enzyme (1.4 mg/mL), and porcine lipase (6 mg/mL). • Incubated at 37 °C for 6 h with shaking.	• Filtered onto aluminium oxide filters (0.02 µm pore size, Anodisc).
Xu et al. [33]	• 1 g of tissue digested in 20 mL of 10% KOH solution at 50 °C for 48 h with agitation (80 rpm). • 3 mL of 30% H_2O_2 added and incubated at 25 °C for 24 h with shaking (80 rpm).	• Ultrapure water and filtered through silver membrane filters (pore size 0.45 µm) using a glass vacuum filtration system.
Song et al. [46]	• Dried at 60 °C to constant weight. • Solvents used: Chloroform, Hexafluoroisopropanol, and Xylene (heated at 150 °C). • Extracts were concentrated at 80 °C.	-
Zhang et al. [38]	• LDIR/SEM: Digested with concentrated nitric acid (25 °C for 46 h, then 60 °C for 3 h). • Py-GC/MS: Dissolved in concentrated nitric acid (40 °C, 48 h).	• For LDIR/SEM: Vacuum-filtered through a stainless steel mesh (pore size 13 µm). • For Py-GC/MS: Filtered with glass fiber membrane.
Li et al. [53]	• Digested in 30% H_2O_2 solution (200 mL) at 65 °C with shaking (80 rpm) for 48 h.	• Vacuum filtration onto mixed cellulose ester membrane filters (47 mm diameter, 5 µm pore size).
Zhang et al. [55]	• LDIR: Digested with concentrated nitric acid (90%). • Py-GCMS: Extracted thrice using chloroform, toluene, and hexafluoroisopropyl alcohol.	• Filtered, rinsed, and ultrasonically treated in ethanol.
Liu et al. [39]	• Digested in concentrated nitric acid (68%) with a tissue-to-solution ratio of 1.0 g: 10 mL. • Shaken continuously at 120 rpm for 3 days at room temperature (25 °C). • Ultrapure Milli-Q water was added to adjust the pH to 1–2.	-

Table 1. *Cont.*

Ref.	Sample Preparation	Filtration
Guo et al. [57]	• Samples dried. • Extracted sequentially with hexafluoroisopropanol, dichloromethane, and xylene via ultrasonication.	-
Tian et al. [8]	• Mixed 2 mL subsample with 4 mL of 15% KOH solution. • Incubated at 40 °C for 48 h with shaking (163 g).	• Filtered through a sterile 0.8 cm^2 glass filter.
Wang et al. [58]	• Dried at 95 °C for 3 h. • Digested with concentrated nitric acid at 95 °C for 3 h.	-
Zhang et al. [59]	• Approximately 0.5 g of endometrial tissue and 2 mL of urine digested with 4 mL of 10% KOH (v/v). • Incubated at 60 °C for 24 h in sealed glass containers.	• Filtrated using sterile glass filters to deposit MPs.
Ren et al. [52]	• Semen homogenized. • Digested with 500 µg proteinase K.	• Filtered through a 1 µm silica membrane.
Özsoy et al. [47]	• Digested using a solution of 30% KOH: NaClO. • Kept on a hot plate at 50 °C for one week.	• Filtered through GF/C filter paper (0.45 µm pore size).
Wu et al. [60]	• Digested using 30% KOH solution at 60 °C for 4 h. • Followed by 48 h at room temperature.	• Filtered through 0.7 µm-pore glass filters.
Peng et al. [13]	• Tissues (approx. 1 g) excised using sterile scalpels. • Digested using 10% KOH solution (48 h at 50 °C) followed by 30% H_2O_2.	• Filtered through silver filter membranes with a 0.45 µm pore size.
Zhang et al. [48]	• Lyophilized (freeze-dried). • Ground with a stainless steel pestle and mortar. • Sieved through a 2 mm stainless steel sieve.	-
Huang et al. [54]	• Treated with concentrated nitric acid (68%) for an hour.	• Vacuum-filtered using a 0.45 µm silver membrane.
Yang et al. [50]	• Tissues: Digested with 30 wt% H_2O_2 (12 h/day for 20 days), followed by 68 wt% HNO_3, and 10 wt% NaOH (for neutralization). • Blood: Collected via PP syringes; received no special pretreatment.	• Filtered through 1 µm PTFE membranes.

Table 1. *Cont.*

Ref.	Sample Preparation	Filtration
Saraluck et al. [28]	• Digested with 10% KOH at 40 °C for 48 h.	• Filtered through a funnel and vacuum pump with a 1.6 µm pore size membrane.
Rotchell et al. [32]	• Digested in 200 mL of 30% H_2O_2 in a shaking incubator at 65 °C. • Incubation for ~7 days or until visible tissue was gone.	• Filtered onto 0.02 µm Anodisc filters using a glass vacuum filtration system.
Shim & Min [61]	• ~20 mL of fluid stirred with 50 mL of 30% H_2O_2. • Incubated for 7 days at 60 °C.	• Filtered through 5 µm silicon filters (10 × 10 mm).
Horvatits et al. [14]	• ~2 cm^3 of tissue weighed. • Rinsed with filtered MilliQ water. • Digested in 30 mL of a 10:1 ratio of KOH and NaOCl for 72 h at 40 °C.	• Stained with Nile Red (1 mg/mL) • Filtrated with Anodisc filters (0.2 µm).
Wang et al. [62]	• Digested with concentrated nitric acid to remove organic matter. • Dried.	-
Deng et al. [63]	• LDIR: Digested with nitric acid. • Py-GC/MS: Extracted using trichloromethane, hexafluoroisopropanol, and xylene.	-
Tokito et al. [7]	• Treated to remove organic particles while preserving MPs' integrity.	• Vacuum filtration through PTFE filter membranes.
Demirelli et al. [10]	• Digested using a 10% KOH solution. • Incubated at 40 °C for 3–5 days to dissolve organic matter.	• Digested suspension filtered through 2.5 µm Whatman filter membranes.
Codrington et al. [9]	• Digested using a solution of potassium hydroxide (KOH), sodium hypochlorite (NaOCl), and a surfactant (Tween-20). • Incubated at 45 °C for 20 h. • Then incubated at 60 °C for 4 h.	• Digested samples filtered.
Pironti et al. [64]	• Organic components removed by digesting urine with a 10% KOH solution (ratio 1:2 sample/KOH). • Incubated for 48 h at 40 °C.	• Vacuum-filtered through 1.2 µm pore-size filter membranes.
Guo et al. [44]	• Digested with enzyme liquid system (proteinase K, SDS, Tris-HCl, $CaCl_2$). • Incubated at 60 °C for 8 h. • Stored at room temperature for 3 days.	• Digested solutions filtered through stainless steel membranes (10 µm pore size). • Particles washed into anhydrous ethanol and ultrasonicated.

3.2. Analytical Identification Techniques

After sample preparation and particle isolation, various analytical techniques are used to identify, characterize, and quantify MPs in human biological samples. Among the most commonly applied methods are Raman spectroscopy, μ-FTIR, LDIR spectroscopy, and Py-GC/MS. Each technique offers distinct advantages in terms of particle size detection, polymer identification, imaging capability, sensitivity, and quantitative analysis. Consequently, recent studies increasingly employ complementary or multimodal analytical approaches to achieve more reliable and comprehensive characterization of MPs in complex biological matrices.

3.2.1. Raman Spectroscopy

Raman spectroscopy is one of the most commonly used techniques for identifying and characterizing MPs in human biological samples. The technique identifies MPs based on the interaction between laser light and plastic particles, producing characteristic spectral fingerprints that help distinguish different polymer types [65]. Due to its high sensitivity, Raman spectroscopy has been widely applied in recent studies investigating human exposure to MPs. Both Raman microscopy and micro-Raman (μ-Raman) spectroscopy have been used to detect MPs in a wide range of tissues and body fluids. Different laser wavelengths, including 532 nm, 633 nm, and 785 nm, were commonly selected depending on the sample type and analytical conditions (Table 2). For example, Xu et al. used micro-Raman spectroscopy with a 532 nm laser to identify MPs in cervical cancer tissues and blood samples [25]. Similarly, Dong et al. applied Raman spectroscopy to detect MPs in female reproductive tissues [27]. Beyond reproductive tissues, Raman-based methods were also used in respiratory and other biological samples. Özgen Alpaydin et al. identified MPs in bronchoalveolar lavage samples collected from patients with interstitial lung disease using μ-Raman spectroscopy [30]. In another study, Montano et al. used Raman microspectroscopy to detect MPs in human semen samples [15]. Raman spectroscopy was also applied for the analysis of MPs in urine [51,64], thrombi [60], placenta [29], and cervicovaginal lavage fluid [61].

One of the major advantages of Raman spectroscopy is its ability to detect very small particles, including MPs smaller than 20 μm [66]. The technique can also provide detailed information about particle size, shape, and polymer composition. In addition, Raman analysis is non-destructive, allowing the same particles to be examined further if needed [67]. However, the method still has some limitations. Biological materials may produce fluorescence signals that interfere with Raman spectra and reduce identification accuracy. The analysis process can also be time-consuming because particles are often examined individually. Moreover, highly degraded plastics may generate weak signals, making polymer identification more difficult [66,68]. Despite these limitations, Raman spectroscopy remains a widely used and reliable technique for the qualitative characterization of MPs in complex human samples.

3.2.2. μ-FTIR

Fourier Transform Infrared (FTIR) spectroscopy, and particularly its microscopic variant (μ-FTIR), is another widely used technique for the identification and characterization of MPs in human biological samples (Table 2). Like Raman spectroscopy, FTIR relies on the interaction of infrared light with chemical bonds, generating characteristic absorption spectra that serve as fingerprints for different polymer types [69]. μ-FTIR is especially valuable for analysing small particles because it combines infrared spectroscopy with optical microscopy, allowing direct visualisation and chemical mapping of MPs in complex sample matrices [70,71].

Several recent studies have successfully applied μ-FTIR and ATR-FTIR to detect MPs in human tissues and body fluids. For example, Jenner et al. used μ-FTIR in transmission mode with a liquid nitrogen-cooled MCT detector (Nicolet iN10) to identify MPs in lung tissue samples from different lobes [31]. Using the same instrument, Leonard et al. detected MPs in human whole blood and reported polymer types, concentrations, and particle size ranges [43]. Rotchell et al. employed μ-FTIR to characterise MPs in human urine from healthy donors and endometriosis patients, as well as in saphenous vein tissue collected during coronary artery bypass grafting [32,72]. Halfar et al. used FTIR-ATR (Nicolet iN10) together with a stereomicroscope to analyse MPs in amniotic fluid and placenta, requiring a spectral match quality above 60% [56]. Min et al. applied μ-FTIR to identify MPs in various nasal samples, including nasopharyngeal fluid, turbinates, and nasal hair [73]. Demirelli et al. used ATR-FTIR spectrophotometry to detect polymers such as polyamide (nylon 6), polypropylene, and polydimethylsiloxane in human prostate tissue [10]. In addition, Huang et al. combined μ-FTIR with LDIR to analyse MPs in sputum samples from the deep lung [54].

A significant strength of μ-FTIR is its non-destructive nature, which allows the same particles to be re-analysed or examined by complementary techniques [74]. It also benefits from extensive spectral libraries that enable reliable polymer identification, especially for larger particles (typically >10 μm) [75,76]. Although extensive spectral libraries facilitate polymer identification, the reliability of μ-FTIR analysis also depends on the choice of reference library, the spectral matching algorithm and threshold, and transparent reporting of these parameters [77,78]. The use of proprietary or laboratory-specific spectral libraries, together with inconsistent reporting of library versions, preprocessing procedures, matching algorithms, and identification thresholds, can hinder reproducibility and inter-study comparability [77]. Recently, curated open-source libraries have emerged to improve transparency and standardization, although their performance still requires careful validation [79]. Moreover, μ-FTIR is less affected by fluorescence interference than Raman spectroscopy, which is a significant benefit when analysing biological samples that often contain autofluorescent components [68]. Nevertheless, μ-FTIR also has limitations. Its spatial resolution is generally lower than that of Raman spectroscopy; particles smaller than about 10 μm are difficult to measure reliably in transmission or reflection mode, although recent advances in synchrotron-based μ-FTIR can push this limit. Water strongly absorbs infrared radiation, so aqueous samples must be thoroughly dried before analysis, which may alter particle morphology or cause loss of volatile components [75]. In addition, like Raman, the manual identification of individual particles under the microscope can be time-consuming, and heavily weathered or degraded plastics may produce spectra that are difficult to match against library references [68,76]. Despite these challenges, μ-FTIR remains a powerful and complementary tool to Raman spectroscopy for the detection and characterisation of MPs in human biological matrices, especially for particles in the micro-size range where both high chemical specificity and spatial visualisation are required.

3.2.3. LDIR Spectroscopy

Laser Direct Infrared (LDIR) spectroscopy is an emerging and increasingly popular technique for the rapid identification and quantification of MPs in human biological samples (Table 2). Laser Direct Infrared Imaging (LDIR) combines a tunable quantum cascade laser (QCL) with an infrared microscope, enabling rapid chemical imaging of particles on a filter surface without conventional point-by-point spectral mapping. The system commonly operates in reflection/transflection or transmission modes over the molecular fingerprint region (~975–1800 cm^{-1}), providing fast and automated polymer-specific characterization [80,81].

Recent studies have increasingly employed LDIR chemical imaging for the detection and characterisation of MPs in diverse human tissues and body fluids. In reproductive and reproductive-associated samples, LDIR has been applied to placental tissues, human semen, and endometrial tissues, enabling the identification of particle size distributions and polymer compositions such as PET, BR, and CPE [26,36,44,52]. Similarly, Zhao et al. used LDIR to quantify MPs in semen and various tumour tissues, including lung, gastric, colorectal, and pancreatic cancers [11,12]. In cancer-related studies, LDIR has also been utilised to analyse MPs in penile cancer tissues, renal cell carcinoma tissues, prostate cancer tissues, and tumour thrombi, often in combination with complementary techniques such as SEM, RNA-seq, and Py-GC/MS [9,37,38,63]. In addition, multimodal analytical workflows integrating LDIR with Py-GC/MS, SEM, or μ-FTIR have been adopted for the investigation of MPs in gallbladder tissue and bile, vitreous humour, sputum, cardiac tissues, and thrombi associated with cardiovascular diseases [35,45,50,54,62].

One of the major advantages of LDIR spectroscopy is its speed. Because it uses a quantum cascade laser (QCL) instead of a broadband IR source, it can rapidly scan entire filter areas and automatically detect and identify particles, often within seconds per particle [82]. The system is capable of detecting MP particles down to approximately 10 μm in size, depending on the optical configuration and workflow. LDIR provides both particle counts and, in some cases, semi-quantitative mass estimates based on particle size and density assumptions. Compared to conventional μ-FTIR, LDIR workflows significantly reduce analysis time and operator-dependent variability through automation [82]. Additionally, the system can streamline sample analysis by reducing manual intervention and minimizing user bias. LDIR is also compatible with commonly used filter substrates such as silver membrane filters, stainless steel meshes, and glass fiber filters [83]. However, LDIR spectroscopy has several limitations, including a practical detection limit of around ~10 μm, making the reliable identification of very small MPs and nanoplastics difficult. In addition, spectral libraries remain less comprehensive than those of μ-FTIR and Raman spectroscopy, while heavily weathered or black particles may produce weak or ambiguous spectra [84]. Despite these limitations and the relatively high instrumentation cost, LDIR remains t a powerful high-throughput technique for rapid MP screening and polymer identification in the ~10–500 μm size range.

3.2.4. Py-GC/MS

Pyrolysis–Gas Chromatography/Mass Spectrometry (Py-GC/MS) is a powerful destructive thermoanalytical technique widely used for the quantitative identification of MPs in human biological samples (Table 2). Unlike spectroscopic techniques such as Raman, μ-FTIR, and LDIR, which depend on optical or chemical imaging of individual particles, Py-GC/MS identifies polymers through thermal degradation. In this technique, polymer macromolecules are pyrolyzed at high temperatures (typically around 400–600 °C) under an inert atmosphere, producing characteristic volatile pyrolysis compounds. These compounds are then separated using gas chromatography and subsequently detected by mass spectrometry, generating unique pyrogram fingerprints that enable reliable polymer identification as well as quantitative determination of polymer mass concentrations [85,86].

Py-GC/MS has been increasingly applied in human biomonitoring studies, frequently in combination with spectroscopic techniques such as LDIR, Raman microscopy, and SEM to provide complementary information on both particle counts and polymer mass concentrations. Recent studies have successfully applied this multimodal approach to a wide range of human biological samples, including gallbladder tissue and bile, vitreous humour, semen, tumour tissues, stool, arteries, bone marrow, amniotic fluid, thrombi, prostate tissues, aqueous humour, tear fluid, and meibum [8,11,12,35,39,45,46,52,57,58,62,63,87].

These studies consistently demonstrated the capability of Py-GC/MS to quantify polymer mass concentrations, commonly reporting polymers such as PE, PP, PS, PVC, PET, and PA66 in units ranging from ng/g to mg/g. In several cases, significantly elevated MP concentrations were observed in diseased tissues compared with control or para-tumour samples, highlighting the potential clinical relevance of MP accumulation. Additionally, tandem mass spectrometry approaches such as LC-MS/MS have also been employed for targeted quantification of specific polymers, including PET and PC, in human stool and meconium samples [48].

One of the major advantages of Py-GC/MS is its ability to determine the absolute mass concentration of polymers rather than only particle counts, which is highly important for exposure and risk assessment studies [88]. The technique also shows high sensitivity toward a broad range of polymers, including weathered, pigmented, and black MPs that are often difficult to detect using optical methods. In addition, Py-GC/MS can simultaneously identify multiple polymer types and, in some cases, associated organic additives or contaminants within a single analysis [89]. Because the sample is completely pyrolyzed, the method avoids particle-by-particle visual selection, thereby reducing operator bias.

However, when Py-GC/MS is applied to complex lipid-rich biological matrices, careful interpretation of pyrograms is essential. Endogenous lipids can generate pyrolysis products that overlap with characteristic polymer markers, particularly those used for polyethylene (PE), thereby increasing the risk of false-positive polymer identification if lipid removal and marker selection are inadequate [90]. This issue has received considerable attention following recent reports of microplastics in human brain tissue, as subsequent methodological evaluations have raised concerns regarding methodological limitations and potential analytical interferences that may affect polyethylene identification in highly lipid-rich samples [91]. Therefore, rigorous lipid removal procedures, the selection of polymer-specific pyrolysis markers, the inclusion of procedural blanks, and complementary confirmation using spectroscopic techniques such as μ-FTIR or Raman microscopy are recommended to improve the reliability and accuracy of polymer identification in biological tissues [90].

Despite these advantages, Py-GC/MS has several limitations. Since it is a destructive technique, samples cannot be reused for further characterization after analysis. Moreover, the method does not provide information on particle size, shape, or colour because the sample is homogenized prior to pyrolysis. Therefore, complementary techniques such as LDIR, μ-FTIR, Raman microscopy, or SEM are often required for morphological analysis. Sample preparation can also be labor-intensive, typically involving digestion of organic matter, filtration, and strict contamination control. Furthermore, the instrumentation is expensive and requires skilled personnel for operation and data interpretation [90]. Quantification additionally depends on suitable polymer-specific calibration standards, which may not always be available. Nevertheless, Py-GC/MS remains one of the most reliable techniques for quantitative MP analysis in environmental and biological samples and is frequently combined with spectroscopic methods to achieve more comprehensive characterization.

Collectively, these analytical techniques provide complementary strengths for comprehensive MP characterization in human biological samples. Raman spectroscopy offers high spatial resolution and superior detection of smaller particles, whereas μ-FTIR provides robust polymer identification with lower fluorescence interference. LDIR enables rapid, automated high-throughput screening of MPs, while Py-GC/MS remains the most reliable approach for quantitative determination of polymer mass concentrations. Therefore, recent studies increasingly combine multiple analytical platforms to achieve more accurate, sensitive, and comprehensive assessment of MPs in complex human matrices (Figure 2). A head-to-head comparison of the major analytical techniques, including their size detec-

tion limits, identification accuracy, throughput, instrumentation cost, and suitability for different sample types, is provided in Supplementary Table S1.

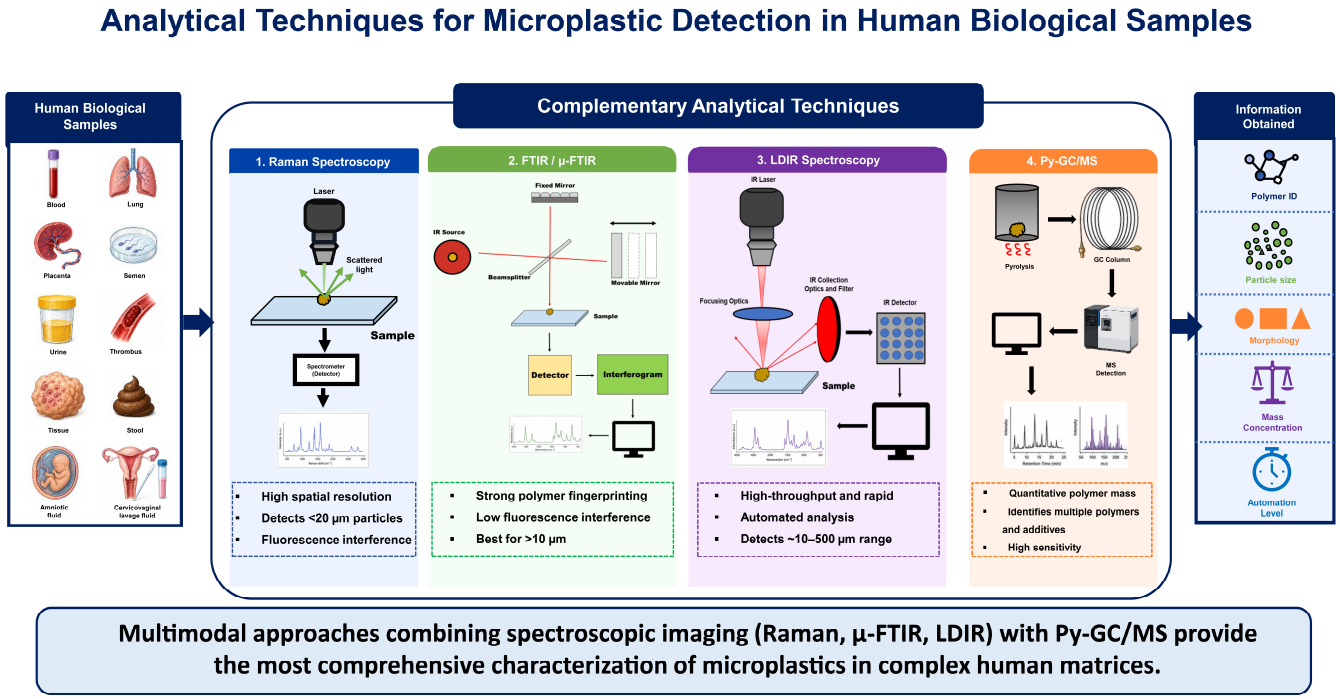


Figure 2. Overview of analytical techniques used for MP detection and characterization in human biological samples.

Table 2. Detection instruments and supporting analytical methods.

Ref.	Samples	Detection/Analytical Methods
Xu et al. [25]	Blood, cancerous tissue	µ-Raman Spectroscopy (RMS) (Laser 532, 200–4000 cm^{-1}).
Wang et al. [26]	Umbilical cord blood	LDIR (Laser Direct Infrared, Agilent 8700). Spectral Range: 900–1800 cm^{-1} (trans-reflection mode). Multivariable regression, BKMR, and quantile g-computation.
Özgen Alpaydin et al. [30]	Broncho Alveolar Lavage (BAL) fluid and blood	µ-RMS (Witec Alpha 300 R) with an excitation value of 532 nm.
Wang et al. [35]	Gallbladder and bile samples	Pyrolysis–gas chromatography/mass spectrometry (Py-GC/MS), LDIR (Particle counting, size distribution 20–500 µm). Scanning Electron Microscopy (SEM).
Halfar et al. [56]	Amniotic fluid and placental tissue	Olympus SZX10 stereomicroscope, FTIR–ATR (Nicolet iN10), Omnic ™ Picta (match >60% required).
Jenner et al. [31]	Lung tissue samples	µ-Fourier Transform Infrared Spectroscopy (µ-FTIR) in liquid nitrogen-cooled transmission mode (Nicolet iN10 with MCT detector).
Zhao et al. [12]	Human Tumor Samples	LDIR (wavenumbers 900–1800 cm^{-1}, match quality > 0.9). Py-GC/MS.
	Human Tumor samples	Py-GCMS, PY-3030D Frontier pyrolyzer coupled with GCMS-QP2020 system; 30 m RTX-5MS column; Helium carrier gas (1 mL/min).
Montano et al. [15]	Human Semen Samples	RMS, Xplora NanoRaman or XploRA (Horiba Scientific). Laser 532 nm or 785 nm; spectral range 500–1800 cm^{-1}.
Sun et al. [36]	Human Endometrial	LDIR spectroscopy (Agilent 8700), Spectral range 900–1800 cm^{-1}.

Table 2. *Cont.*

Ref.	Samples	Detection/Analytical Methods
Zong et al. [45]	Human Vitreous Humor	LDIR Agilent 8700 system, Py-GC/MS, SEM
Wang et al. [37]	Normal tissue and Cancer tissue from Human Penile Cancer Patients	LDIR spectroscopy (Agilent 8700 system), Spectral range 1800–900 cm^{-1} (initial scan) and 900–1800 cm^{-1} (trans-reflection).
Kim et al. [92]	Human Endometrial Tissue	LDIR, SEM.
Rotchell et al. [72]	Human Urine	Inverted fluorescence microscope, Intracellular Reactive Oxygen Species (ROS) assay kit (DCFH-DA). FITC-Annexin V-FITC/PI staining.
Dong et al. [27]	Patient of Adenomyosis, ovarian ectopic cyst, uterine tube removal	Micro RMS (LabRAM HR Evolution), Scanning range 4000 cm^{-1} to 600 cm^{-1}.
Montano et al. [49]	Human Ovarian Follicular Fluid	SEM, SEM-EDX (X-ray Energy-Dispersive Spectroscopy) coupled with AZTEC Version 5.1 software, Detection Limit: LOD of 0.1 µm and LOQ of 0.3 µm;
Ragusa et al. [29]	Human Placenta	µ = RMS (Horiba Scientific Raman XploRA Nano). Laser at 532 nm; Spectral range 400–2000 cm^{-1}.
Massardo et al. [51]	Human Renal and Urine samples	µ-RMS (Renishaw System 2000 coupled with Leica light microscope). He-Ne 633 nm laser; 500× magnification (detection down to ~1 µm); spectral range 4000–100 cm^{-1}. SpeComp (open-access).
Leonard et al. [43]	Whole blood	Nicolet™ iN10 Infrared Microscope in liquid nitrogen-cooled transmission mode. Spectral Parameters: Range 4000–1250 cm^{-1}, resolution 8 cm^{-1}, 64 scans.
Xu et al. [33]	Human Uterine fibroid and Myometrium	LabRAM HR Evolution (HORIBA Jobin Yvon S.A.S). 532 nm laser; spectral range 200–4000 cm^{-1}; 50× long working distance objective.
Song et al. [46]	Human Stool	Py-GC/MS (Frontier Lab EGA/PY-3030D coupled with Shimadzu GC-2030 and QP2020 MS).
Zhang et al. [38]	Human renal and inferior venacava	DIR & SEM. RNA-seq.
Li et al. [53]	Human Synovium	Stereomicroscopy, µ-FTIR (Nicolet iN10 MX, 4000–600 cm^{-1}, transmittance mode). RMS (Renishaw inVia Reflex, 600–1800 cm^{-1}, 785 nm laser). SEM (S-4800). RNA-seq.
Zhang et al. [55]	Human gallstone and Mice	Agilent 8700 LDIR, Shimadzu GCMS-QP2020 system, Fluorescence Imaging: Leica DM2500 microscope. 16S r-RNA gene sequencing.
Liu et al. [39]	Human Coronary, Aortic and Carotid Artery samples	Py-GC/MS. Frontier Lab Py-3030D pyrolyzer coupled with Shimadzu GCMS-QP 2020.
Guo et al. [57]	Human Bone Marrow	Py-GC/MS, LDIR (Detection range 20–500 µm), SEM.
Tian et al. [8]	Human Amniotic Fluid	RMS with 785 nm laser, spectral range 500–1500 cm^{-1}. Py-GC/MS: Shimadzu GCMS-QP 2020 Plus coupled with Frontier Lab pyrolyzer.
Wang et al. [58]	Human Tear fluid and Meibum	LDIR with spatial resolution of 0.25 µm. SEM, Py-GC-MS.
Zhang et al. [59]	Human Urine and Endometrial Samples	RMS with 785 nm laser, spatial resolution 0.25 µm, spectral range 500–1500 cm^{-1}. Py-GC/MS.
Ren et al. [52]	Human Sperm Samples	LDIR (Particle size range 20–500 µm; matching degree > 0.65).
Özsoy et al. [47]	Human Stomach	Olympus microscope, Spectroscopy: µ-Raman analysis (Renishaw in via Qontor) using 532 nm and 785 nm lasers.
Wu et al. [60]	Thrombi samples	Raman Spectrometer (LabRAM HR Evolution) with a 785 nm diode laser and 600 lines/mm diffraction grating.

Table 2. *Cont.*

Ref.	Samples	Detection/Analytical Methods
Peng et al. [13]	Uterine Tissue samples	Micro-confocal Raman spectrometer (HORIBA Jobin Yvon) with a 532 nm solid-state laser.
Zhang et al. [48]	Meconium, Infant and adult faeces	Tandem Mass Spectrometry (LC-MS/MS).
Min et al. [73]	Nasal hair sample	μ-FTIR (Thermo Scientific Nicolet iN10 microscopy).
Huang et al. [54]	Sputum	Micro-FTIR, LDIR: Agilent 8700.
Yang et al. [50]	Venous Blood Samples	Agilent 8700 LDIR chemical imaging system. Size Range: 20–500 μm.
Saraluck et al. [28]	Postpartum breast milk	Olympus microscope, micro RMS (spectral range 200–1800 cm^{-1}; lasers: 532, 638, 785 nm), 16S r-RNA sequencing.
Rotchell et al. [32]	Urine	μ-FTIR spectrometer (Nicolet iN10, Thermo Fisher) in liquid nitrogen-cooled transmission mode.
Shim & Min [61]	Human cervicovaginal lavage fluid	RMS using an XploRA Plus Confocal Raman microscope. 532 nm laser, 1200 grooves/mm grating, 1024 × 256 pixel detector, Spectral range 1020–3400 cm^{-1}, 1 × 2 s exposure.
Horvatits et al. [14]	Liver tissue (cirrhotic and non-cirrhotic), kidney tissue, spleen tissue	Fluorescence Microscopy, RMS: μ- RMS (Thermo Fisher DXR2xi) with 532 nm and 785 nm lasers.
Wang et al. [62]	Thrombus	Py-GC/MS, LDIR, SEM.
Deng et al. [63]	Prostate tissue (para-tumor and tumor)	LDIR: Agilent 8700 LDIR, SEM, Py-GC/MS.
Zhang et al. [87]	Human Aqueous humor	Py-GC/MS.
Tokito et al. [7]	Broncho Alveolar Lavage fluid	Nile Red Staining/Fluorescence Microscopy (excitation 460 nm, emission 525 nm). μ-RMS with 532 nm laser.
Demirelli et al. [10]	Prostate tissue	Light Microscopy, ATR-FTIR Spectrophotometry.
Codrington et al. [9]	Penile tissue (corpus cavernosum)	LDIR Chemical Imaging: Agilent 8700 LDIR, Zeiss Merlin SEM.
Pironti et al. [64]	Human Urine	μ-RMS: XploRA Nano Raman Micro spectrometer with 532 nm or 785 nm laser.
Guo et al. [44]	Semen	LDIR Spectroscopy, Agilent 8700 LDIR system using trans-reflection mode.

4. Distribution of MPs in Human Biological Samples

Recent advances in analytical technologies have enabled the detection of MPs across a wide range of human biological samples, providing growing evidence of their widespread distribution within the human body. Studies have reported MPs in various body fluids, tissues, and organs, suggesting that exposure occurs through multiple pathways, including ingestion, inhalation, and dermal contact. The reported abundance, size distribution, morphology, and polymer composition of MPs vary considerably among sample types and study populations. Nevertheless, the repeated detection of common polymers such as PE, PP, PS, PET, and PVC highlights the pervasive nature of human exposure.

Before accumulating in internal organs and biological fluids, MPs must traverse one or more biological barriers that normally regulate the movement of endogenous and exogenous substances [93]. Current evidence suggests that MPs may cross biological barriers, including the intestinal epithelium, blood–placenta barrier, blood–testis barrier, blood–retinal barrier, and glomerular filtration barrier, although the precise mechanisms remain incompletely understood [1,94]. Experimental studies have proposed that particle

translocation may occur through pathways such as endocytosis, transcytosis, paracellular transport, or barrier disruption associated with oxidative stress and inflammation [94–96]. The efficiency of barrier penetration appears to depend on several physicochemical characteristics of MPs. Smaller particles generally exhibit greater translocation potential than larger particles, whereas particle morphology, polymer composition, and surface properties, including the formation of a biomolecular (protein) corona, may further influence cellular uptake, tissue interactions, and biodistribution [97–99]. Nevertheless, direct evidence in humans remains limited because current analytical techniques are largely optimized for microplastics rather than NPs, and methodological heterogeneity continues to hinder a comprehensive understanding of barrier penetration and internal translocation. Therefore, further mechanistic investigations and standardized analytical approaches are required to clarify how different particle characteristics influence the movement of MPs across biological barriers. The following sections summarize current evidence regarding the occurrence and distribution of MPs in human biological fluids, tissues, and organs.

4.1. MPs in Human Fluids

Human body fluids provide valuable insight into the transport, circulation, accumulation, and potential elimination of MPs within the body (Table 3). Because many biological fluids are directly connected to organ systems and physiological barriers, their analysis offers important information regarding internal exposure pathways and the movement of MPs between different anatomical compartments. Recent studies have identified MPs in a variety of fluids, including blood, amniotic fluid, breast milk, semen, ocular fluids, lavage fluids, urine, stool, and meconium. Together, these findings suggest that MPs can circulate throughout the body and may reach both peripheral tissues and highly protected biological environments.

Table 3. MP types, sizes, colors, and concentration/abundance in human body fluids, excreta, and lavage-related samples.

Human Body Fluid		Ref.	MP Type	Size and Color	Concentration
Blood	Whole Blood	Xu et al. [25]	Dominant: PE (26.44%), PE-co-PP (19.54%), PP (14.94%). Others: PU, PMMA, Rubber, PEVA, PLY, PS-co-PVC, PVAc, PS, PPS, PA	Length: Avg 20.03 μm, Width: Avg 15.93 μm	2.2 ± 1.42 items/mL (Detection Rate: 80%)
		Leonard et al. [43]	PE (32%), EPDM (14%), EVA/EVOH (12%), PA, Nylon, Acrylic, PET, PP, PS, PVC, Polyurethane (PUR), Resins, etc.	Length: Range: 7–3000 μm), Width: Range: 5–800 μm, White (41%), Clear (38%)	2466 ± 4174 MP/L, 0.66 ± 0.87 μg/mL, PE: 4.65 μg/mL EPDM: 2.22 μg/mL EVA/EVOH: 1.84 μg/mL
	Peripheral Blood	Özgen Alpaydin et al. [30]	PA (50%), PE (50%)	13.14 μm–20.29 μm, Grey/White (50%), Blue (50%)	Particles: 100.0%
	Venous Blood (Pre-Surgery)	Yang et al. [50]	Dominant: PA (49%), PET (22%)	Range: 20–184 μm, Predominantly 30–50 μm (67% of MPs)	
	Venous Blood (Post-Surgery)		Dominant: PA (57%), PET	Range: 20–184 μm, Predominantly 20–30 μm (51% of MPs)	
	Thrombi (Arterial Blood Clot)	Wu et al. [60]	LDPE, Phthalocyanine, Hostasol-Green G-K	Range: 2.1–26.0 μm, <10 μm: 69%, Mars Red, Mars Yellow, Green	Total Count: 87 identified particles (23 synthetic), Particles per Thrombus: Range: 1–15 particles

Table 3. *Cont.*

Human Body Fluid		Ref.	MP Type	Size and Color	Concentration
Lavage Fluid	Bronchoalveolar Lavage (BAL)	Özgen Alpaydin et al. [30]	Dominant (20% each): PA, PET, PVC, PU. Others: PAM, PC	4.19 µm–792.00 µm, Grey/White (46.7%), Black (33.3%), Others: Red/Pink, Blue	ILD Group: 55.6% (10/18), Control Group: 28.6% (2/7)
	Cervicovaginal Lavage Fluid (CVF)	Shim & Min [61]	Predominant: PP (73.8%), PS (10.1%), Others: PE, PET, PMMA	Range: 5–100 µm, 10–20 µm: 41.8%, 20–50 µm: 26.4%, 5–10 µm: 22.0%, 50–100 µm: 9.9%	Mean Concentration: 9.10 ± 14.96 particles/10 g, Range: 0–51 particles/sample
	Bronchoalveolar Lavage Fluid (BALF)	Tokito et al. [7]	Dominant: PVC (25.5%), PS (19.1%), PET (12.8%), PP (8.5%). Others: PMMA, Cellulose, Nylon, PE	Median: 3.29 µm (Range: 1.21–261.7 µm), 81.5% of particles <10 µm	Median Concentration: 684.7 particles/mL
Urine		Rotchell et al. [72]	Healthy: PE (27%), PS (16%), Resins (12%), PP (12%). Endometriosis: PTFE (59%), PE (16%)	Healthy: Mean length 61.9 µm, Width 34.9 µm (Range 19–400 µm). Clear/White (89%).	Healthy: 2589 ± 2931 MP/L (Unadjusted). Endometriosis: 4724 ± 9710 MP/L (Unadjusted)
		Massardo et al. [51]	PE, PS, Styrene-Isoprene (Rubber), Hematite, Cu-phthalocyanine	Range: 3 µm–13 µm, Red/Orange, Light/Dark Blue	Visual Particles Found: 23 Spectroscopically Identified: 7 particles
		Zhang et al. [59]	PTFE (24.2%), PS (60.6%), PC, PE, PVC	Range: 1.23–6.36 µm, Mean: 2.85 ± 1.26 µm	
		Pironti et al. [64]	PVA, PVC, PP, PE	Range: 4–15 µm. Transparent, Brown, Blue, Grey, Green, Red, Orange, Yellow	Females: 1 positive (2 particles), Males: 3 positive (5 particles)
Reproductive Fluid	Semen	Zhao et al. [12]	PE (25%), PVC (25%), PA (17%), PS (13%), PP (13%), PET (7%)	Avg: 96.19 ± 74.17 µm, Range: 21.76–286.71 µm, Predominant: 20–100 µm (67% of particles)	Avg: 0.23 ± 0.45 particles/mL Range: 0–2.06 particles/mL Avg: 15.34 ± 23.31 µg/mL Range: 0.098–56.188 µg/mL
		Montano et al. [15]	PP, PS, PET, PE, POM, PVC, PC, Acrylic	2–6 µm, Green, Black, Grey, Orange, Blue, transparent, Magenta	16 fragments, 0–5 MPs per sample (Mean: 1.6 MPs/sample)
		Ren et al. [52]	CPE, PVC, PS, PE, PU, PSF	Range: 20–500 µm	Mean Concentration: 104 ± 53.58 particles/g
		Guo et al. [44]	Dominant: PET (35.9%), BR (26.4%), CPE (12.2%), PP	Range: 20–189.7 µm, Mean: 53.0 ± 31.9 µm, 20–50 µm: 60.0%, 50–100 µm: 33.2%, 100–150 µm: 7.4%, 150–200 µm: 1.6%	Mean: 17.0 ± 42.0 particles/g, Median: 3.9 particles/g. Abundance by Polymer (Mean particles/g): PET: 6.1 (±38.8), BR: 4.5 (±11.6), CPE: 2.1 (±4.9), PP: 1.2 (±3.5)
	Ovarian Follicular Fluid (FF)	Montano et al. [49]	PS	Mean Diameter: 4.48 µm, Range: 3.18–5.54 µm, Red	Mean Concentration: 2191 particles/mL, Range: 0–7181 particles/mL
	Amniotic Fluid	Tian et al. [8]	PTFE (31.25%), PS (20.83%), ABS (14.58%), PE (10.42%), PC (2.08%), PVC (2.08%)	Average: 3.05 ± 1.05 µm, Range: 0.94–5.73 µm, Dominant: Black, Others: Brown, Red	
		Halfar et al. [56]	CPE, PE, PE-HD, PET, PU, PP, Polyester	6.8 µm–260 µm, most frequent size: 20 –50 µm	Median: 1 particle per patient, Range: 0–8 particles, Max Concentration: 1.6 items/mL

Table 3. *Cont.*

Human Body Fluid		Ref.	MP Type	Size and Color	Concentration
Nasal Samples	Nasopharyngeal Fluid (NF), Inferior Turbinate (IT), Nasal Hair (NH), Middle Turbinate (MT), Middle Nasal Cavity Fluid (MNCF)	Min et al. [73]	Dominant: PE, Polyester, Acrylic Polymer, PP. Others: PS, PS Copolymer, PE–PP Copolymer, PU, Polysulfone, PVC, PE Copolymer, PHB, PVC Copolymer Fragments: 90.77%, Fibers: 9.23%	Overall Average: Width: 29.43 ± 15.49 µm, Length: 57.14 ± 51.98 µm	Total Count: 390 MPs. NF: 129, IT: 93, NH: 86, MT: 51, MNCF: 31
Stool	Human Stools (Fecal samples)	Song et al. [46]	PE (Most dominant), PVC, PS, PP, PET, PA66		Overall Median: 54.7 µg/g (Range: 10.1–102.7 µg/g) By Polymer (Median: µg/g): PE: 20.3, PVC: 16.3, PS: 1.3
	Meconium (Newborn Stool), Infant Stool (1-year-olds), Adult Stool	Zhang et al. [48]	PET, PC		Newborn Stool: PET: <LOQ–12,000 ng/g dw, PC: <LOQ–110 ng/g dw, Infant Stool: PET: Range: 5700–82,000 ng/g dw, PC: Range: 49–2100 ng/g dw, Adult Stool: PET: Range: <LOQ–16,000 ng/g dw, PC: Range: 37–620 ng/g dw
Eye Fluid	Vitreous Humor (Eye Fluid)	Zong et al. [45]	Dominant Polymers: Nylon 66 (PA66), PS, PVC. Others: PE, PP, PMMA, PA6	20–500 µm, 20–50 µm: 63.8%, 50–500 µm: 36.2%	Macular Epiretinal Membrane: 14.76 mg/kg (PA66), 1.38 mg/kg (PS), 0.67 mg/kg (PVC) Macular Hole: 12.32 mg/kg (PA66), 0.70 mg/kg (PS), 0.24 mg/kg (PVC) Retinopathy: 9.14 mg/kg (PA66), 0.81 mg/kg (PS), 0.81 mg/kg (PVC) Retinal Detachment: 11.63 mg/kg (PA66), 0.83 mg/kg (PS)
	Tear Fluid	Wang et al. [58]	Dominant: PE, PS, Others: PVC, PP, PC, PA66, ABS, PTFE, EVA, PMMA, PBAT	Range: 20–500 µm, 20–100 µm: 71.27%, Dominant: Black, Others: Brown, Red	Mean Concentration (µg/g): PE: 24.13 ± 17.69, PVC: 19.09 ± 15.65, PS: 6.76 ± 5.87, PP: 2.04 ± 2.35
	Aqueous Humor (Eye Fluid)	Zhang et al. [87]	Predominant: PE, PVC, Others: PP (Predominant in children), PA66 (Primarily in adults), PS		Overall Concentration (mg/g): Adults: 13.5943 ± 5.5322, Children: 11.0485 ± 4.7926, Elders: 6.7508 ± 3.4429. Females: 13.0909 ± 5.8658, Males: 7.8381 ± 2.9850

Table 3. *Cont.*

Human Body Fluid		Ref.	MP Type	Size and Color	Concentration
Other	Bile	Wang et al. [35]	BR (~37.0%), SBS (~27.8%), PE (~10.8%), Others: SIS, PP, PIB	20–500 µm, 20–50 µm: ~70%, 50–100 µm: ~20%, >100 µm: ~10%	Avg: 118 particles/sample (Range: 100–135), PE: Avg 12.9 µg/g
	Meibomium (Meibomian gland)	Wang et al. [58]	Dominant: PE, PVC, PS, Others: PP, PC, PA66, ABS, PTFE, EVA, PMMA, PBAT, PA6, PET, PU	-	Mean Concentration (µg/g): PE: 23.86 ± 25.28, PVC: 15.21 ± 18.65, PS: 5.56 ± 2.74, PP: 0.54 ± 1.13
	Stomach (Duodenum Contents)	Özsoy et al. [47]	PE (30.5%), PP (13.9%), PMMA (13.9%), PA (11.1%), PET/Polyester (11.1%)	Range: 51.53–4789.1 µm, Fibers: 1196.6 ± 907.1 µm, Films: 635.6 ± 310.8 µm, Fragments: 330.4 ± 261.4 µm, Blue (38.8%), Black (24.5%), Transparent (11.2%), Red (11.2%)	Average per Individual: 9.4 ± 10.4 particles, Estimated Daily Intake: ~32.2 particles/person/day
	Human Breast (Breast Milk)	Saraluck et al. [28]	Prevalent Polymers: PP, PE, PS, PVC, Others: PA, PET	Dominant: Dark Brown, Black. Others: Blue, Green, Red, Pink, Yellow, Gray	Particles per Sample: 1 polymer: 13 samples, 2 polymers: 6 samples, 3 polymers: 3 samples, 4 polymers: 1 sample
	Sputum (Deep Lung)	Huang et al. [54]	Dominant: PU (33.95%), PES (21.63%), CPE, Alkyd Varnish. Others: Acrylates, Acrylonitrile Butadiene, EVA, Polyacetal, PE, Polyimide, PVC, Rubber, Silicone, PC, PTFE	Range: 20–500 µm, Median: 75.43 µm, IQR: 44.67–210.64 µm	Total MPs: Median 39.5 particles/10 mL Polymer Abundance (Median particles/10 mL): PU: 8 (3.25–10.75), PES: 5 (0–19.25), CPE: 4.5 (0–10.75), Alkyd Varnish: 2.5 (0–15)

4.1.1. Somatic Fluids

Somatic fluids have emerged as important biological matrices for understanding the distribution of MPs within the human body. Since these fluids circulate throughout different organs and tissues, they may facilitate the transport, accumulation, and possible elimination of MPs from multiple anatomical compartments. Evaluating the size, abundance, color, and polymer composition of MPs in body fluids may therefore provide important insights into exposure patterns, vulnerable populations, and their possible association with disease development (Table 3). Recent studies have detected MPs in several human body fluids, including amniotic fluid, breast milk, ocular fluids, and respiratory-associated fluids, using complementary analytical approaches. In amniotic fluid, Halfar et al. identified MPs mainly composed of chlorinated polyethylene (CPE), PE, PET, PU, and PP using FTIR-ATR [56], while Tian et al. reported a high detection rate using Raman spectroscopy and Py-GC/MS, with PTFE, PS, and ABS being the dominant polymers [8]. These findings demonstrate the presence of MPs in both maternal and fetal compartments, indicating potential prenatal exposure. Similarly, Saraluck et al. detected MPs in 38.98% of breast milk samples, primarily consisting of PP, PE, and PVC, indicating possible neonatal exposure during early developmental stages [28]. MPs have also been identified in ocular and respiratory-related fluids. Wang et al. detected predominantly PE particles in tear fluid and meibum from dry eye patients [58], whereas Zhong et al. and Zhang et al. reported MPs in vitreous and aqueous humor, respectively, suggesting that ocular barriers may not completely prevent MP accumulation [45,87]. In respiratory-associated samples, Min et al. identified 390 MP particles across different nasal and nasopharyngeal sites, with PE, polyester, acrylic polymer, and PP being the most common polymers [73]. Across these studies, most detected MPs were relatively small, commonly below 50 µm, which may

enhance their ability to cross biological barriers and circulate within body fluids. Variations in MP abundance were also observed according to age and sex. Zhang et al. reported higher MP levels in adults and females, while Min et al. observed differences in dominant polymer types between children and adults, suggesting possible age-dependent exposure patterns [73,87]. Overall, these findings indicate that MPs can circulate through the human body and accumulate in multiple somatic fluid compartments, supporting their systemic distribution following environmental exposure. The repeated detection of polymers such as PE, PP, PVC, and PS across different matrices is consistent with widespread human exposure to plastics commonly encountered in food packaging, textiles, bottled water, and household products. Particularly concerning is the presence of MPs in amniotic fluid and breast milk, as these findings indicate potential fetal and neonatal exposure during critical developmental stages. Recent human observational and cohort studies have highlighted the potential clinical relevance of MPs detected in maternal and neonatal biological samples, including the placenta, amniotic fluid, breast milk, and meconium. Their presence across these maternal–fetal biological matrices suggests that fetal exposure to MPs may begin before birth, although the biological consequences remain uncertain [100]. However, the current human evidence is largely observational and remains insufficient to establish a causal relationship between gestational MP exposure and adverse pregnancy or neonatal outcomes. Several observational studies have reported that higher placental MP burden is associated with lower birth weight and reduced 1 min Apgar scores. In addition, meconium microplastics have been associated with reduced microbiota diversity, suggesting that prenatal MP exposure may influence early neonatal health [101]. Recent evidence has also shown that MP abundance in amniotic fluid is inversely associated with gestational age, indicating that fetal exposure may vary throughout pregnancy [102]. Differences in the distribution of MPs across placental tissues at different gestational stages have been reported; however, these findings should be interpreted cautiously because of small sample sizes, methodological heterogeneity, and the lack of standardized analytical protocols [100]. Overall, the available evidence supports the need for large, prospective longitudinal cohort studies using standardized sampling and analytical methods to clarify the relationship between gestational MP exposure, placental accumulation, and neonatal developmental outcomes. Ocular studies additionally suggest possible associations between MP accumulation and ocular surface disorders, including dry eye disease [45,58]. These observations further suggest that somatic fluids may serve as valuable indicators for monitoring human MP exposure and understanding their movement within the body. However, the long-term biological fate, clearance pathways, and potential cumulative effects of MPs in these fluid compartments remain poorly understood and warrant further investigation. Collectively, despite differences in sample type and study population, the available evidence demonstrates a consistent pattern of MP occurrence across diverse somatic fluids. This observation further supports the widespread distribution of MPs across multiple biological compartments. Although the reported polymer profiles varied among studies, PE and PP were the most consistently identified polymers, suggesting widespread human exposure irrespective of sample type. The detection of MPs in protected biological fluids, particularly amniotic and ocular fluids, further highlights their widespread distribution and suggests that MPs may reach these compartments following environmental exposure, raising concerns regarding their long-term biological implications. While current evidence confirms the widespread presence of MPs in somatic fluids, whether their accumulation directly contributes to disease development or primarily reflects environmental exposure remains unclear. Therefore, future mechanistic and longitudinal studies are needed to clarify the biological significance of these findings.

4.1.2. Reproductive Fluids

Reproductive fluids such as semen and ovarian follicular fluid are increasingly being investigated for MP contamination because of their importance in gamete function and fertility. Recent studies using LDIR, Raman microspectroscopy, Py-GC/MS, and SEM have confirmed the presence of MPs in human semen, testis, and ovarian follicular fluid (Table 3). Zhao et al. detected MPs in 11 of 25 semen samples and all examined testis samples, with PS dominating in testis, whereas PVC and PE were more common in semen [11]. Similarly, Ren et al. reported a 100% detection rate in semen samples, identifying CPE, PVC, and PS as predominant polymers [52]. In female reproductive samples, Montano et al. found MPs in 14 of 18 ovarian follicular fluid samples, with particles averaging only 4.48 μm in diameter and reaching high concentrations (2191 particles/mL) [49]. Across reproductive tissues, MPs were predominantly small in size, although detected ranges varied depending on analytical techniques. LDIR studies commonly identified particles within the 20–100 μm range, whereas Raman spectroscopy detected much smaller particles (2–6 μm) [11,15,52]. Fragments were the dominant shape in testis, while semen contained mixed morphologies including fragments, fibers, and films. The detection of MPs in both testis and follicular fluid suggests that these particles can be detected in protected reproductive tissues, potentially affecting reproductive physiology. Consistent with these observations, higher MP levels in follicular fluid were positively associated with increased FSH levels [15], while experimental studies have demonstrated that PS exposure can induce mitochondrial ROS generation, sperm damage, and embryonic abnormalities [52]. Overall, these findings indicate that MPs can accumulate within human reproductive environments and may influence reproductive physiology. Moreover, the predominance of small-sized particles across semen, testis, and ovarian follicular fluid suggests an enhanced capacity to penetrate biological barriers and persist within sensitive reproductive tissues. The consistent detection of MPs in both male and female reproductive fluids strengthens the evidence that these particles can access highly protected reproductive environments. Unlike somatic fluids, where MPs primarily reflect systemic distribution, their presence in semen, testis, and ovarian follicular fluid is of greater biological relevance because these tissues are directly involved in gamete function and early embryonic development. Although the available human studies provide only associative evidence, their findings are supported by experimental studies demonstrating oxidative stress, mitochondrial dysfunction, and impaired sperm function following MP exposure. Collectively, these observations suggest that the reproductive system may represent one of the most biologically vulnerable targets of MPs. However, current human evidence remains insufficient to determine whether MPs are causally involved in infertility or other adverse reproductive outcomes.

4.1.3. Blood

As the primary circulatory compartment, blood provides an important biological matrix for investigating the systemic transport and internal distribution of MPs. Investigating the abundance and size distribution of MPs in blood can provide valuable insights into their movement and deposition across different organs. Furthermore, such studies may help to elucidate potential exposure–disease relationships, systemic health risks, and the possible translocation of plastic particles within the human body (Table 3). Recent studies using μ-FTIR, LDIR, Raman spectroscopy, and Py-GC/MS consistently detected MPs in human blood samples, with PE, PP, PET, and PA among the most frequently identified polymers. Using micro-Raman spectroscopy, Xu et al. detected MPs in 80% of whole blood samples collected from cervical cancer patients, with PE, PE-co-PP, and PP as the predominant polymers [25]. The average particle size was relatively small, measuring approximately 20 μm in length and 16 μm in width, while the mean concentration reached

2.2 ± 1.42 items/mL. Similarly, Özgen Alpaydin et al. reported a 100% detection rate in peripheral blood samples, although only two polymer types, PA and PE, were identified [30]. The detected particles ranged from 13–20 µm and were primarily grey/white or blue in colour. In contrast, Leonard et al. employed µ-FTIR spectroscopy and identified a much broader spectrum of polymers, including PE, EPDM, EVA/EVOH, PET, PP, PS, PVC, PUR, and acrylic materials [43]. Particle sizes showed substantial variability, ranging from 7 µm to 3000 µm in length, with fragments and transparent or white particles dominating the samples. Their estimated MP concentration reached 2466 ± 4174 MP/L, alongside measurable polymer mass concentrations, indicating that blood may carry a substantial plastic burden even in apparently healthy individuals. Evidence from surgical patients further supports the dynamic circulation of MPs within the bloodstream. Using LDIR analysis, Yang et al. identified PA and PET as dominant polymers in venous blood collected before and after cardiac surgery [50]. Although the particle size range remained similar (20–184 µm), post-surgical samples showed a shift toward smaller particles, with most MPs falling within the 20–30 µm range. These findings suggest that medical procedures may represent an additional source of MP exposure, although the underlying mechanisms and their clinical significance remain uncertain. Taken as a whole, the consistent detection of MPs across independent blood studies indicates that their presence in the circulation is unlikely to represent isolated findings. Although the reported particle concentrations, size ranges, and polymer profiles varied among studies, PE and PET were repeatedly identified, suggesting that these polymers constitute a substantial proportion of circulating MPs. As blood connects virtually all organs, its role extends beyond reflecting internal exposure and may facilitate the systemic transport of MPs to secondary tissues. However, while circulating MPs have been hypothesized to contribute to inflammatory and cardiovascular processes, current human evidence remains largely observational and does not establish a direct causal relationship. Therefore, blood may serve as a valuable biomarker of internal MP exposure, whereas the long-term biological consequences of persistent circulation and tissue deposition require further investigation.

4.1.4. Gastrointestinal System

The gastrointestinal system is considered a major entry and processing route for human exposure to MPs, as ingested and inhaled particles may undergo accumulation, fragmentation, degradation, and systemic translocation within the digestive tract. Recent studies have confirmed the presence of MPs in both stomach and biliary samples, highlighting their potential role in gastrointestinal and hepatobiliary pathophysiology (Table 3). Ozsoy et al. provided the first direct evidence of MPs in the human stomach using µ-Raman spectroscopy following chemical digestion and density separation of stomach contents collected from 26 cadavers [47]. MPs were detected in all individuals, with PE, PP, PMMA, Nylon-6, and PET/polyester identified as the predominant polymers. Particle sizes ranged from approximately 51 µm to 4789 µm, with fibers representing the dominant morphology, followed by fragments and films. A strong skew toward smaller particles suggested that MPs below the analytical threshold (~50 µm) were likely underrepresented. Compared with previously reported stool burdens, the lower gastric MP load suggested ongoing gastric clearance, fragmentation, and degradation processes within the stomach. The predominance of fibers and the detection of large particles further support the gastrointestinal tract as a dynamic environment where MPs may undergo physical and chemical transformation before excretion or absorption. Evidence of MPs within the biliary system further expands the understanding of MP distribution within digestive organs. Wang et al. [35] analyzed gallbladder tissue and bile samples from patients undergoing surgery for gallstones or gallbladder polyps using Py-GC/MS, LDIR, and SEM. Multiple polymer types

were identified, with PE, PA66, and PVC being the most abundant. LDIR analysis revealed 9–11 polymer types per sample, with most particles ranging between 20 and 50 μm. Average particle counts reached 51.8 particles in gallbladder tissue and 118 particles in bile samples, indicating substantial MP accumulation within the biliary environment. Interestingly, sex-associated differences were observed for PVC, PP, and PA66 distribution, while PE abundance remained relatively comparable between males and females. The coexistence of MPs with cholesterol-rich gallstones suggested that MPs may act as nucleation sites that facilitate crystal aggregation and gallstone formation through adsorption of bile acids and cholesterol onto their hydrophobic surfaces. These findings raise the possibility that enterohepatic circulation and dietary exposure contribute to MP persistence within the gallbladder and bile. Thus, these findings indicate that the gastrointestinal tract is not merely a passage route but also a site where MPs may undergo physical breakdown and potentially translocate to bile and beyond.

4.1.5. Lavage Fluid

Lavage fluids have emerged as valuable and minimally invasive matrices for investigating local exposure and accumulation of MPs within the respiratory and reproductive systems. In particular, bronchoalveolar lavage fluid (BALF) and cervicovaginal lavage fluid provide insight into how MPs interact with epithelial barriers, inflammatory environments, and mucosal tissues. Recent studies employing Raman-based analytical techniques have consistently confirmed the presence of MPs in these lavage samples, supporting concerns regarding both respiratory and reproductive exposure pathways (Table 3). In BAL fluid, Özgen Alpaydin et al. employed μ-Raman spectroscopy to compare patients with interstitial lung disease (ILD) and healthy controls [30]. MPs were detected in 55.6% of ILD patients and 28.6% of controls, with PA, PET, PVC, and PU identified as the dominant polymers. Particle sizes varied widely, ranging from 4.19 μm to 792 μm, while grey/white and black particles predominated morphologically. Similarly, Tokito et al. analyzed BALF using Nile Red staining, fluorescence microscopy, and micro-Raman spectroscopy and identified PVC, PS, PET, and PP as the major polymers [7]. Most detected particles were notably small, with over 80% measuring below 10 μm and a median size of 3.29 μm, indicating that fine MPs can penetrate deeply into the lower respiratory tract. The reported median concentration of 684.7 particles/mL further suggests substantial MP accumulation within pulmonary lavage samples. In reproductive lavage samples, Shim and Min investigated CVF using Raman spectroscopy and reported PP as the predominant polymer, followed by PS, PE, PET, and PMMA. Most particles ranged between 10 and 50 μm, although smaller particles within the 5–10 μm fraction were also frequently observed [61]. The average MP concentration was 9.10 ± 14.96 particles per 10 g of sample, with marked interindividual variability among participants. Across lavage fluid studies, PVC, PS, PET, PP, and PA were among the most frequently detected polymers. While BAL samples demonstrated a particularly high abundance of smaller MPs, CVF samples showed predominance of mid-sized particles within the 10–50 μm range. The consistent detection of MPs in both respiratory and reproductive lavage fluids suggests that plastic particles can access deep pulmonary tissues through inhalation and may also accumulate within the cervicovaginal environment through direct local exposure, including potential contribution from feminine hygiene products. Across the available studies, the findings from both bronchoalveolar and cervicovaginal lavage samples indicate that MPs can accumulate at mucosal surfaces directly exposed to the external environment. The predominance of small particles in BALF and comparatively larger particles in CVF further suggests that particle size and exposure route may influence local deposition patterns. Although current evidence confirms localized MP ex-

posure, its contribution to chronic mucosal inflammation or disease progression remains to be clarified.

4.1.6. Excretory Waste

Excretory waste represents an important biological matrix for assessing human exposure to MPs and understanding their potential elimination pathways. Unlike many internal tissues and fluids, excretory samples can be collected non-invasively and may reflect both recent and long-term exposure to environmental plastics. Studies investigating stool, meconium, and urine have consistently detected MPs of various sizes and polymer compositions, providing evidence that plastic particles can enter the gastrointestinal and urinary systems and subsequently be excreted. Evaluating MPs in excretory waste therefore offers valuable insight into exposure patterns, internal processing, and the possible clearance of MPs from the human body.

Stool and Meconium

Stool and meconium represent non-invasive matrices that reflect dietary exposure to MPs and fetal exposure, respectively. Recent studies have consistently identified MPs in adult stool, infant stool, and meconium, supporting the widespread presence of plastic particles within the human excretory system (Table 3). Song et al. analyzed stool samples from young adults using Py-GC/MS and identified PE as the predominant polymer, followed by PVC, PS, PP, PET, and PA66 [46]. The overall median MP concentration reached 54.7 μg/g, indicating considerable variation in MP burden among individuals. Similarly, Zhang et al. quantified PET and polycarbonate (PC) in adult stool, infant stool, and meconium using tandem mass spectrometry [48]. Notably, infant stool contained substantially higher PET concentrations compared with adult stool, while measurable levels of PET and PC were also detected in meconium samples. The detection of MPs in meconium is particularly significant, as it suggests that plastic particles can reach the fetal gastrointestinal tract before birth through maternal–fetal transfer pathways. Across stool and meconium studies, PE, PET, and PC were among the most frequently detected polymers. The markedly elevated PET levels reported in infant stool compared with adult samples may reflect differences in feeding practices, including formula preparation and bottle feeding, as well as immature gastrointestinal clearance mechanisms during early life. These findings collectively indicate that exposure to MPs may begin during fetal development and continue throughout infancy and adulthood through dietary and environmental sources. The differences observed between adult stool, infant stool, and meconium further suggest that age, dietary habits, and developmental stage may substantially influence MP burden and excretion patterns. Overall, stool analysis represents a practical and non-invasive approach for monitoring population-level MP exposure and gastrointestinal elimination. The consistent detection of MPs across adult, infant, and neonatal samples further highlights the pervasive nature of plastic exposure and raises concerns regarding long-term accumulation and early-life vulnerability to MP-associated health effects.

Urine

Recent studies have identified urine as a promising biological fluid for investigating the systemic distribution and possible elimination of MPs in humans (Table 3). The repeated detection of MPs in urinary samples suggests that sufficiently small plastic particles may circulate throughout the body and eventually reach the renal or urinary system following environmental exposure.

Rotchell et al. [13] analyzed urine samples from healthy donors and individuals with endometriosis using μ-FTIR spectroscopy and detected MPs in most samples from both groups [72]. PE, PS, and PP were the predominant polymers in healthy individuals, whereas

PTFE was particularly abundant in endometriosis-associated urine. The study also reported relatively large particle dimensions compared with Raman-based investigations, with mean particle lengths exceeding 60 µm in healthy donors and 100 µm in endometriosis samples. In contrast, Raman spectroscopy-based studies consistently identified smaller MPs. Pironti et al. first demonstrated the presence of MPs in urine from Italian volunteers, identifying coloured fragments composed of PVA, PVC, PP, and PE [64]. Similarly, Massardo et al. detected PE- and PS-associated particles ranging from 3–13 µm, while Zhang et al. reported even smaller MPs in postpartum urine samples, with PS and PTFE as dominant polymers and an average particle size of approximately 3 µm [51,59]. Across urinary studies, PE, PS, PP, and PTFE were among the most frequently detected polymers. Irregular fragments represented the dominant morphology, and most particles measured below 50 µm. The predominance of smaller particles supports the possibility that only micrometric MPs may pass through the glomerular filtration barrier or enter the urinary tract through systemic circulation. Reported MP abundance varied markedly between studies, ranging from only a few detected particles to several thousand particles per litre, likely reflecting differences in analytical sensitivity, sampling procedures, and contamination control strategies. Interestingly, the prominent detection of PTFE in endometriosis-associated urine but not in most healthy samples raises questions regarding disease-associated exposure patterns or altered retention and clearance mechanisms. At the same time, the frequent detection of common environmental polymers such as PE, PS, and PP further supports dietary and inhalational exposure as likely contributors to urinary MP burden. Taken together, urinary studies suggest that the detection of MPs is influenced not only by environmental exposure but also by particle size, as smaller particles appear more likely to reach the urinary tract following systemic circulation. Although polymer composition and reported abundance differed among studies, the repeated identification of PE, PS, PP, and PTFE supports the view that urinary MPs are a consistent finding rather than isolated observations. Nevertheless, whether urinary MPs primarily reflect renal clearance, local urinary tract exposure, or disease-associated alterations remains uncertain and warrants further investigation.

Overall, the available evidence indicates that the route of exposure is a key determinant of the initial uptake and subsequent systemic distribution of microplastics (MPs), although the relative contribution of each pathway is influenced by particle characteristics and biological transport mechanisms [103]. Collectively, the findings presented in this section support the view that ingestion and inhalation are likely the principal contributors to systemic MP exposure, whereas dermal absorption appears to contribute minimally under normal physiological conditions because intact skin provides an effective biological barrier [103]. Following ingestion, a proportion of smaller MPs may translocate across the intestinal epithelium via M-cell-mediated uptake, endocytosis, or paracellular transport before entering the portal or lymphatic circulation, resulting in initial hepatic exposure and, based primarily on experimental evidence, subsequent redistribution to other organs. Conversely, inhaled MPs that reach the alveolar region may traverse the alveolar–capillary barrier and enter the bloodstream, whereas larger particles are predominantly removed through mucociliary clearance and subsequently swallowed, thereby linking respiratory and gastrointestinal exposure pathways [103]. Following systemic entry, physicochemical properties, including particle size, shape, polymer composition, surface chemistry, and interactions with biological molecules (e.g., protein corona formation), collectively influence biological barrier penetration, tissue distribution, and organ-specific accumulation in organs such as the liver, kidneys, placenta, reproductive organs, and potentially the brain. Nevertheless, despite increasing evidence of MP detection in multiple human tissues, most human biomonitoring studies identify MPs only at the site of accumulation without determining their original route of entry, and simultaneous exposure through multiple

pathways further complicates source attribution. Consequently, although current evidence supports plausible mechanistic links between exposure routes and organ distribution, the relative contribution of ingestion, inhalation, and dermal contact to the overall systemic MP burden remains insufficiently resolved, emphasizing the need for integrated human exposure assessment, toxicokinetic investigations, and biodistribution studies to better define route-specific organ accumulation. To improve cross-study comparison and enhance the readability of the evidence presented in Table 3, a statistical summary of the reported findings, including the number of studies, predominant polymer types, particle characteristics (size and color), and concentration patterns across different human biological fluids, is provided in Supplementary Table S2.

Because the included studies reported MP concentrations using heterogeneous units (e.g., particles/mL, particles/g, μg/g, and mg/kg) and different analytical techniques with varying detection limits, direct quantitative comparisons across biological compartments were not feasible. Therefore, the reported concentrations should be interpreted cautiously, and standardized reporting methods are needed to facilitate future comparative analyses.

4.2. MPs in Human Tissues and Organs

Recent studies have confirmed the presence of MPs in multiple human tissues and organs, including the placenta, lungs, reproductive tissues, blood vessels, liver, kidney, heart, and tumour tissues. Most detected particles were small in size and commonly composed of polymers such as PE, PP, PS, PET, and PVC, suggesting their ability to penetrate and accumulate within biological tissues. Although the health effects are still not fully understood, growing evidence indicates possible associations between MP accumulation and inflammation, oxidative stress, tissue damage, and various human diseases.

4.2.1. Uterus and Endometrium Tissue

The uterus and endometrium are among the most extensively studied human tissues for MP detection, with multiple studies confirming the presence of MPs in endometrial tissue, uterine fibroids, myometrium, adenomyosis lesions, uterine tubes, and endometrial stromal cells (Table 4). A broad range of polymers, including PE, PP, PS, PET, PVC, PTFE, PU, ABS, and PE-co-PP, were identified across these tissues. Most detected particles were relatively small, commonly below 100 μm, while some studies reported particles as small as 1–5 μm [59]. The predominance of small-sized particles is particularly important because smaller MPs are more likely to penetrate biological barriers, accumulate within tissues, and interact directly with cells. Different particle shapes, such as fibres, fragments, films, and microspheres, were also observed, suggesting multiple environmental and consumer-related exposure sources [33]. Several studies reported higher MP concentrations in diseased reproductive tissues compared to healthy tissues. Xu et al. found greater MP accumulation in uterine fibroids than in healthy myometrium, while Peng et al. observed significantly elevated MP levels in fibroids, endometrial cancer, and cervical cancer tissues [13,33]. Similarly, MPs were consistently detected in adenomyosis tissues, ovarian ectopic cysts, and uterine tubes [27]. Although these findings do not establish a direct causal relationship, they suggest a possible association between long-term MP exposure and gynaecological disorders. The ability of MPs to adsorb endocrine-disrupting chemicals and environmental pollutants may further contribute to hormonal imbalance and tissue abnormalities within the female reproductive system. Importantly, Kim et al. demonstrated that polystyrene micro- and nanoparticles could enter both the cytoplasm and nucleus of endometrial stromal cells [92]. This finding indicates that very small plastic particles may directly interfere with cellular processes, potentially contributing to oxidative stress, inflammation, apoptosis, and DNA damage. Together, these studies provide growing evidence

that MPs can accumulate in reproductive tissues and may influence female reproductive health at both tissue and cellular levels. However, due to differences in analytical methods, sample preparation, and reporting units among studies, further standardized investigations are needed to clarify the long-term health implications and underlying mechanisms of MP-related reproductive toxicity.

Table 4. MP types, sizes, colors, and concentration/abundance in human solid tissues, cells and organs.

Human Body	Reference	Human Body Tissue	MP Type	MP Size and Color	Concentration
Female Reproductive	Xu et al. [25]	Cancerous Tissue (Cervical)	Dominant: PE (26.44%), PE-co-PP (19.54%), PP (14.94%). Others: PU, PMMA, Rubber, PEVA, PLY, PS-co-PVC, PVAc, PS, PPS, PA	Length: Avg 21.48 μm, Width: Avg 14.91 μm	1.67 ± 0.94 items/g (Detection Rate: 80%)
		Paracancerous Tissue (Normal/Adjacent)	Dominant: PE (26.44%), PE-co-PP (19.54%), PP (14.94%). Others: PU, PMMA, Rubber, PEVA, PLY, PS-co-PVC, PVAc, PS, PPS, PA	Length: Avg 23.25 μm, Width: Avg 16.98 μm	0.87 ± 0.72 items/g (Detection Rate: 66.67%)
	Sun et al. [36]	Human Endometrium (Functional layer)	EAA (34.6%), FR (14.87%), CPE (11.47%), PE (9.95%), ACR (7.76%), PU (7.76%), PET, PP, PS, PVC, BR, EVA, Phenolic epoxy resin	20–500 μm, 20–100 μm (88.35%), 100–500 μm (11.65%)	Median: 21 particles/100 mg, 0–117 particles/100 mg
	Kim et al. [92]	Endometrial Stromal Cells (ESCs)	PS	NPs: 100 nm, MPs: 1 μm. Green, Yellow	Nuclear Uptake: (FL)PS-MPs: 79.1 ± 5.9%, (FL)PS-NPs: 67.8 ± 8.9%. Cytoplasmic Uptake: (FL)PS-MPs: 20.9 ± 6.8%, (FL)PS-NPs: 24.8 ± 7.4%
	Dong et al. [27]	Adenomyosis Tissues (AT), Ovarian Ectopic Cysts (OEC), Uterine Tubes (UT)	Dominant: PE (31%), PP (22%), PE-co-PP (11%). Others: PS (8%), PET (7%), PA (6%), PU (5%), PEVA (3%), ABS (3%), PC (2%), PVAc (2%)	Length: 4.51–26.73 μm, Width: 4.12–26.73 μm, ~70% of MPs were <20 μm, Blue, Light Blue, Brown, Grey	AT: Mean: 1.35 ± 1.06 MP/g, OEC: Mean: 1.45 ± 1.17 MP/g, UT: Mean: 1.40 ± 1.11 MP/g
	Xu et al. [33]	Uterine Fibroids (UFs), Myometrium (from UF Patients), Myometrium (Healthy Volunteers)	Dominant: PE (46.2%), PP (19.2%), PE-co-PP (15.4%). Others: PEVA, PA, ABS, Cotton Fibers (7.7%) s/g. Shapes: Fibers (46.2%), Fragments (30.8%), Films (11.5%), Microspheres (11.5%)	Length: Range: 4.86–40.15 μm, Width: Range: 2.79–22.79 μm, Brown (34.6%), Blue (30.8%), Grey (19.2%), Others: Light white, Dark brown, Yellow, White	Uterine Fibroids: All Samples: 2.13 ± 1.17 particles/g, Matched Patients (Diseased): 2.63 ± 1.77 particles/g. Myometrium: All Samples: 0.88 ± 0.78 particles/g, Matched Patients (Normal): 1.08 ± 0.93 particles/g
	Zhang et al. [59]	Endometrial Tissue	PTFE (51.7%), PS (34.5%), PC, PE, PVC	Range: 1.46–6.98 μm, Mean: 2.89 ± 1.40 μm	—
	Peng et al. [13]	Diseased Uterine Tissues (Fibroids, Endometrial Cancer, Cervical Cancer)	Predominant: PE (18.0%), PP (12.9%), PS (8.6%). Others: PET, PA, PVC, PE-co-PP, PU, PMMA, EAA, ACR, FR, PC, ABS, PLA	Length: 4.69–52.53 μm, Width: 2.92–42.1 μm, Blue, Grey, Brown, Red, Orange, Transparent	Mean Concentration: 3.0 ± 1.53 particles/g, Range: 0–6 particles/sample

Table 4. *Cont.*

Human Body	Reference	Human Body Tissue	MP Type	MP Size and Color	Concentration
Placenta	Wang et al. [26]	Placenta (Maternal and fetal regions)	Dominant: PVC, PP, PBS	10–100 µm (Most frequent), 100–200 µm, >200 µm	Total: 12 particles/10 g (Median)
	Halfar et al. [56]	Placenta	CPE, PE, PE-HD, PET, PU, PP, Polyester, Paper with polymer coating, Zinc Molybdate, Vinyl Ester	6.8–260 µm, most frequent size: 20–50 µm	Median: 2 particles per patient, Range: 0–10 particles, Max Concentration: 20 items/g
	Ragusa et al. [29]	Placenta (Fetal side, Maternal side, Chorionic villi, Decidua basalis, Chorioallantoic membrane)	PP, PET, PVC, Cellulose	Range: ~10–30 µm, Red (Iron oxide), Blue, Yellow, Pink, White (Zinc Oxide), Purple (Ultramarine Blue), Orange, Violet, Grey, Brown	Fetal side: 4 MPs, Maternal side: 3 MPs, Chorionic villi and Maternal side: 2 MPs, Decidua basalis: 1 MP, Chorioallantoic membrane: 2 MPs
Respiratory	Jenner et al. [31]	Lung Tissue (Upper, Middle/Lingular, Lower Lobes)	Dominant: PP (23%), PET (18%), Resin (15%). Others: PE, PTFE, PS, PUR, PMMA, PAN, PES, PVA, SEBS, TPE	Length: 12–2475 µm, Width: 4–88 µm.	Upper Lobe: 0.80 ± 0.96 MP/g, Middle/Lingular Lobe: 0.41 ± 0.37 MP/g, Lower Lobe: 3.12 ± 1.30 MP/g.: Male: 2.09 ± 1.54 MP/g, Female: 0.36 ± 0.50 MP/g
	Zhao et al. [12]	Lung Cancer Tissue	PS, PVC, PE	—	Mean Concentrations (ng/g): PS: 59.56 ± 89.15, PVC: 23.83 ± 38.14, PE: 13.59 ± 14.96
Cardiovascular	Liu et al. [39]	Coronary Arteries (With plaques), Carotid Arteries (With plaques), Aorta (Without plaques)	PET (73.7%), PA-66 (15.54%), PVC (9.69%), PE (1.07%)	—	Coronary Arteries: Mean: 156.50 ± 42.14 µg/g, Carotid Arteries: Mean: 133.37 ± 60.52 µg/g, Aorta:
	Yang et al. [50]	Cardiac Tissues (Pericardium, EAT, PAT, Myocardium, LAA)	Dominant: PET (77%), PU (12%), Others: PE, PA, PC, PS, PVC, PMMA	Range: 20–469 µm	—
	Rotchell et al. [32]	Saphenous Vein (CABG Tissue)	Dominant: Alkyd Resin (45%), PVAc (20%), Nylon-EVA Tie Layer (20%), Other: PUR	Length: Mean: 119.59 ± 226.82 µm, Range: 16–1074 µm, Width: Mean: 41.27 ± 62.80 µm, Range: 7–300 µm	Unadjusted Mean: 29.28 ± 34.88 MP/g (Range: 0–96 MP/g), Blank-Subtracted Mean: 14.99 ± 17.18 MP/g
	Wang et al. [62]	Cerebral Arteries (Ischemic Stroke)	Py-GC/MS: PA66, PVC, PE. LDIR: PE (53.6%), ACR (14.8%), PP (14.3%)	Range: 20–500 µm, 20–50 µm: 84.6%, 50–100 µm: 14.3%, 100–500 µm: 1.1%	Mass Concentration: Median: 61.75 µg/g, Range: 14.88–221.8 µg/g
	Wang et al. [62]	Coronary Arteries (Myocardial Infarction)	Py-GC/MS: PA66, PVC, PE	—	Mass Concentration: Median: 141.80 µg/g, Range: 49.3–234.3 µg/g
		Deep Veins (DVT—Lower Extremities)	Py-GC/MS: PA66, PVC, PE	—	Mass Concentration: Median: 69.62 µg/g, Range: 23.8–94.2 µg/g
	Zhang et al. [38]	Tumor Thrombus (Inferior vena cava)	PE, PS	—	Highest abundance of PE and PS followed by tumor tissue, then normal tissue.

Table 4. *Cont.*

Human Body	Reference	Human Body Tissue	MP Type	MP Size and Color	Concentration
Renal/Urinary	Massardo et al. [51]	Kidney (Tissue from Nephrectomies)	PE, PS, Titanite ($CaTiSiO_5$), Hematite, Cu-phthalocyanine, Cerulean blue	Range: 1 µm–29 µm, White, Red/Orange/ Black, Light/Dark Blue, Black/Grey	Visual Particles Found: 43. Spectroscopically Identified: 19 particles
	Zhang et al. [38]	Carcinoma (Tumor Tissue)	Dominant: PE, PVC, PS, PP, Other: FKM, PET	Range: 20–500 µm	Status: Significantly higher levels than normal tissue. Particle Abundance: Higher than normal tissue.
	Zhang et al. [38]	Normal Renal Tissue (Adjacent)	Dominant: PE, PP, Other: FKM, PET, PVC	Range: 20–500 µm	Status: Significantly lower levels than tumor tissue. Particle Abundance: Lower than tumor tissue.
Gastrointestinal and Hepatobiliary	Wang et al. [35]	Gallbladder Tissue	PE (~55.0%), ABS (~15.7%), EVA (~8.9%), PET (~7.2%), Others: PP, BR	20–500 µm, 20–50 µm: 71.2%, 50–100 µm: 18.6%, >100 µm: 10.2%	Avg: 51.8 particles/ sample (Range: 41–62), PE: Avg 13.2 µg/g
	Zhang et al. [55]	Human Gallstones	PS, PE, PET, PP, EVA	Range: 0–30 µm	PS: 10.69 ± 10.56 mg/kg, PE: 3.56 ± 3.21 mg/kg, PET: 0.18 ± 0.38 mg/kg, PP: 0.09 ± 0.14 mg/kg, EVA: 0.04 ± 0.08 mg/kg
	Zhao et al. [12]	Gastric Cancer Tissue	PS, PVC, PE	—	Mean Concentrations (ng/g): PVC: 78.23 ± 109.23, PS: 27.21 ± 12.86, PE: 18.87 ± 19.16
		Colorectal Cancer Tissue	PS, PVC, PE	—	Mean Concentrations (ng/g): PS: 41.10 ± 32.54, PE: 23.53 ± 12.68, PVC: 9.00 ± 18.90
		Pancreatic Cancer Tissue	PS, PVC, PE	—	Mean Concentrations (ng/g): PS: 128.73 ± 138.45, PVC: 29.98 ± 28.25, PE: 21.01 ± 14.96
Male Reproductive	Zhao et al. [12]	Human Testis (Tissue)	PS (67.7%), PVC (12.9%), PE (12.9%), PP (6.5%)	Avg: 83.15 ± 56.25 µm, Predominant: 20–100 µm (80.6% of particles)	Avg: 11.60 ± 15.52 particles/g
	Deng et al. [63]	Tumor Tissues (Prostate Cancer)	Py-GC/MS: PS, PE, PP, PVC. LDIR: PA, PET, PVC, PE, PS	Range: 20–100 µm, ~35.21% of particles were 50–100 µm	Mass Concentration (Mean): 290.3 µg/g
		Para-tumor Tissues (Non-cancerous)	Py-GC/MS: PS, PE, PP, PVC. LDIR: PA, PET, PVC, PP	Range: 20–100 µm, ~31.58% of particles were 20–30 µm	Mass Concentration (Mean): 181.0 µg/g
	Demirelli et al. [10]	Prostate Tissue	Polyamide (Nylon 6), Polypropylene, Polyacrylic Acid, Polydimethylsiloxane	Range: <26 µm	Particle Count: Average 21.5 ± 10.13 particles/ sample, Tissue Mass: Mean 1.73 g (Range: 0.58–5.27 g)
	Wang et al. [37]	Penile Cancer Tissue (CT)	Dominant: PE, PP, PVC. Others: PA, PMMA, POM, PU, PS, PC.	20–500 µm; Predominant: 20–50 µm	Mean: 7.43 ± 3.70 MPs/g, Total Count: 1745 particles (20 samples)
	Wang et al. [37]	Adjacent Normal Tissue (ANT)	PE, PP, PVC, PA, POM, PU	20–500 µm; Predominant: 20–30 µm	Mean: 5.07 ± 3.70 MPs/g
	Codrington et al. [9]	Penile Tissue (Corpora Cavernosa)	Dominant: PET (47.8%), PP (34.7%)	LDIR Range: 20–500 µm, SEM Range: 2–20 µm, 20–100 µm: 84%	—

Table 4. *Cont.*

Human Body	Reference	Human Body Tissue	MP Type	MP Size and Color	Concentration
Musculoskeletal and Other	Li et al. [53]	Synovium (Hip and Knee Joints)	Dominant: PET (27.1%), PE (21.9%), RA (12.0%), PES (11.1%), PP (9.3%). Others: PA (8.5%), PVC (4.7%), PS (4.4%), PC (2.0%)	Range: 11.00–151.00 µm, Mean: 50.01 ± 22.07 µm. Distribution: <50 µm: 52.2%, 50–80 µm: 35.3%, >80 µm: 12.5%, Blue (21.9%), Transparent (20.7%), White (20.4%)	Overall Mean: 5.24 ± 2.07 particles/g. Hip: 6.35 ± 1.95 particles/g. Knee: 4.79 ± 1.92 particles/g
	Guo et al. [57]	Bone Marrow (Iliac Spine)	Py-GC/MS: PE, PS, PVC, PA66, PP, LDIR: FKM (27.45%), PU (11.27%), CPE (10.78%), PET (9.80%)	Range: 20.34–499.4 µm. <100 µm: 89.82%, 20–50 µm: 71.27%, 50–100 µm: 18.55%, >100 µm: 10.18%	Py-GC/MS: Mean: 51.29 µg/g, Range: 15.37–92.05 µg/g. LDIR: Mean: 19.72 particles/g, Range: 12.27–28.44 particles/g
	Horvatits et al. [14]	Liver (Cirrhotic), Liver (Healthy Control)	PS, PVC, PET, PMMA, POM, PP	Range: 3.0–29.5 µm, Median: 9.8 µm	Liver (Cirrhotic): Median: 3.2 particles/g, Range: 0.3–11.9 particles/g. Liver (Healthy Control): Median: 0.0 particles/g, Range: 0.0–1.5 particles/g

4.2.2. Placenta

The placenta is one of the most studied human tissues for MP detection because it plays an essential role in nutrient and oxygen exchange between the mother and fetus. Several studies summarized in Table 4 confirmed the presence of MPs in placental tissues, indicating maternal exposure and the possible movement of plastic particles across the placental barrier. MPs were identified in different parts of the placenta, including the maternal side, fetal side, chorionic villi, decidua basalis, and chorioallantoic membrane, showing that these particles can spread throughout placental compartments [26,29,56]. Placental samples contained a diverse range of polymer types across different studies. In a recent investigation, Wang et al. reported PVC, PP, and PBS as the major polymers [26]. Similarly, Katharina Halfar et al. identified several polymers, including chlorinated polyethylene (CPE), polyethylene (PE), high-density polyethylene (PE-HD), polyethylene terephthalate (PET), polyurethane (PU), polypropylene (PP), and polyester. Their study also reported materials associated with polymer coatings, such as paper with polymer coating, zinc molybdate, and vinyl ester [56]. In another study, Ragusa et al. detected PP, PET, PVC, and cellulose in placental samples. Beyond polymer composition, Antonio Ragusa et al. also reported the presence of coloured particles and associated additives in placental samples, including red, blue, yellow, pink, white, purple, orange, violet, grey, and brown particles [29]. The observed colour diversity may be attributed to different pigments and additives associated with the detected microplastics, reflecting their heterogeneous composition and possible environmental or industrial origins. Most MP particles identified in placental tissues were relatively small, generally measuring below 100 µm, although reported particle sizes ranged from approximately 6.8 µm to 260 µm depending on the study design and analytical methods used. The most frequently detected particle size range was 20–50 µm [56], while Ragusa et al. additionally reported particles measuring 10–30 µm on the fetal side of the placenta [29]. The presence of MPs in the placenta is particularly concerning because the placenta acts as the connection between maternal and fetal circulation. Detection of MPs in this organ suggests possible fetal exposure and raises concerns about inflammation, oxidative stress, and disruption of normal placental functions. Wang et al. suggested that placental MP exposure may be associated with altered fetal liver enzyme levels, possibly due to oxidative stress or inflammatory responses.

Ragusa et al. proposed that MPs could affect immune responses at the maternal–fetal interface and may contribute to metabolic abnormalities. They also suggested that MPs likely reach the placenta through maternal exposure via the respiratory and gastrointestinal systems. Although the exact health effects are still not fully understood, the repeated detection of MPs in placental tissues across different studies strongly indicates continuous maternal exposure and systemic distribution of plastic particles in humans.

4.2.3. Lung Tissue

The lung is considered one of the major target organs for MP exposure because humans are continuously exposed to airborne particles through inhalation from both indoor and outdoor environments. Several studies summarized in Table 4 have confirmed the presence of MPs in human lung tissues, raising concerns regarding their potential impact on respiratory health.

In a detailed investigation, Jenner et al. analyzed tissues collected from different lung regions, including the upper, middle/lingular, and lower lobes, using μ-FTIR spectroscopy in transmission mode. Their study identified a broad range of polymer types, among which polypropylene (PP) was the most abundant (23%), followed by polyethylene terephthalate (PET) (18%) and resin (15%). Additional polymers detected included polyethylene (PE), polytetrafluoroethylene (PTFE), polystyrene (PS), polyurethane (PUR), polymethyl methacrylate (PMMA), polyacrylonitrile (PAN), polyester (PES), polyvinyl alcohol (PVA), styrene-ethylene-butylene-styrene (SEBS), and thermoplastic elastomers (TPE). The detected particles showed substantial size variation, ranging from 12–2475 μm in length and 4–88 μm in width. Interestingly, MP concentrations differed across lung regions, with the lower lobe containing the highest concentration, followed by the upper lobe and the middle/lingular lobe. The authors also observed sex-related differences, reporting significantly higher MP concentrations in males compared to females [31]. Similarly, Zhao et al. investigated MPs in lung cancer tissues using Py-GC/MS and reported polymer concentrations on a mass basis. Among the detected polymers, polystyrene (PS) showed the highest concentration, followed by polyvinyl chloride (PVC) and polyethylene (PE) [12]. Unlike particle-count-based studies, this approach provided quantitative information regarding the mass accumulation of MPs in lung tissues.

4.2.4. Arteries and Veins

Several studies have reported the presence of MPs in human vascular tissues, including coronary arteries, carotid arteries, the aorta, saphenous veins, cerebral arteries, and deep veins (Table 4). MPs were detected in both atherosclerotic plaques and thrombotic vessels from patients with cardiovascular diseases such as myocardial infarction, ischaemic stroke, and deep vein thrombosis [32,39,62]. The identified polymers included PET, PE, PVC, PA66, PP, PVAc, PUR, alkyd resin, and ACR [25,39,42]. PET was the dominant polymer in coronary and carotid arteries [39], while alkyd resin and PVAc were more common in saphenous vein tissues [32]. Most particles ranged between 20–500 μm, with smaller particles (20–50 μm) being the most frequently detected in thrombotic samples [62]. Coronary arteries generally showed higher MP concentrations compared to other vascular tissues. The detection of MPs in arteries and veins is concerning because these particles may interact with blood vessels and thrombotic tissues. Their accumulation in plaques and thrombi suggests a possible association with vascular inflammation, endothelial damage, and cardiovascular diseases. However, it is still unclear whether MPs directly contribute to disease development or preferentially accumulate in already damaged tissues. Further studies are needed to clarify the underlying mechanisms and long-term health effects of vascular MP exposure.

4.2.5. Brain Tissue

Brain tissue has recently emerged as an important biological matrix for investigating the biodistribution of micro- and nanoplastics (MNPs). Using complementary analytical techniques, including pyrolysis–gas chromatography/mass spectrometry (Py-GC/MS), attenuated total reflectance Fourier transform infrared spectroscopy (ATR-FTIR), and scanning electron microscopy coupled with energy-dispersive spectroscopy (SEM-EDS), Nihart et al. detected MNPs in post-mortem human brain tissue, with polyethylene identified as the predominant polymer and higher concentrations observed in the brain than in paired liver and kidney samples [104]. The study also reported higher MNP burdens in individuals with documented dementia; however, these findings should be interpreted cautiously because the cross-sectional study design does not permit conclusions regarding causality or temporal relationships. Subsequently, methodological concerns were raised regarding the interpretation of Py-GC/MS data in lipid-rich brain tissue. Monikh et al. [91]. noted that residual lipids may generate pyrolysis products overlapping with polyethylene-specific markers, potentially contributing to false-positive or inflated estimates if rigorous lipid removal, contamination control, polymer-specific marker selection, and orthogonal analytical confirmation are not incorporated [91]. Therefore, although the detection of MNPs in human brain tissue raises important questions regarding their ability to cross the blood–brain barrier and their potential involvement in neuroinflammatory or neurodegenerative processes, the current human evidence remains preliminary and insufficient to establish causal relationships with disorders such as Alzheimer's or Parkinson's disease. Future studies employing standardized analytical workflows, multimodal validation, and longitudinal clinical designs are needed to determine the extent of brain accumulation and its potential neurological significance.

4.2.6. Other Human Tissues and Organs

In addition to the placenta, lungs, reproductive tissues, and vascular system, MPs have also been detected in several other human tissues and organs, including the testis, gallbladder, kidney, bone marrow, heart, liver, synovium, prostate, penile tissue, gallstones, and multiple cancer tissues such as gastric, colorectal, pancreatic, renal, and penile tumours (Table 4). Across these studies, commonly detected polymers included PE, PP, PS, PET, PVC, PA, PU, ABS, and PMMA, although the dominant polymer types varied depending on the tissue and analytical method used. Most detected particles were relatively small, frequently below 100 μm, while some studies identified particles as small as 1–5 μm or even nanoscale materials, suggesting a strong potential for tissue penetration and cellular interaction [14,51]. Several studies reported higher MP accumulation in diseased tissues compared to adjacent healthy tissues. For example, renal tumour tissues, prostate cancer tissues, penile cancer tissues, and cirrhotic liver samples generally showed greater MP abundance than corresponding non-diseased tissues [14,37,38,63]. Similarly, MPs were consistently detected in tumour-associated thrombi, gallstones, and inflamed or degenerative tissues such as synovium and bone marrow [39,53,57]. These findings suggest that MPs may preferentially accumulate in damaged or metabolically active tissues, although it remains unclear whether MPs contribute directly to disease development or accumulate secondarily in diseased environments. The detection of MPs in organs, such as the liver, kidney, heart, bone marrow, and testis, is particularly concerning because these tissues are highly vascularized and play critical roles in metabolism, immunity, circulation, and reproduction. Small particle sizes and the presence of chemically active polymers raise concerns regarding oxidative stress, inflammation, endocrine disruption, immune dysfunction, and cellular toxicity. Studies on penile, prostate, and testicular tissues also suggest that MPs may affect male reproductive health [9–11,37,63]. Meanwhile, the identification of MPs in synovial tissues and bone

marrow indicates that plastic particles can distribute widely throughout the body and persist in deep internal tissues.

Therefore, these studies collectively demonstrate that MP contamination is not limited to a few isolated organs but is widespread across multiple human tissues (Figure 3). Although methodological differences among studies affect direct comparisons of concentrations and polymer profiles, the repeated detection of MPs in both healthy and diseased tissues strongly supports the idea of chronic systemic exposure and bioaccumulation in humans. Further standardized studies are needed to better understand the mechanisms of tissue accumulation and the long-term health consequences of MP exposure. To facilitate cross-study comparison and improve the readability of the evidence presented in Table 4, a statistical summary of the reported findings across different human tissues and organs is provided in Supplementary Table S3.

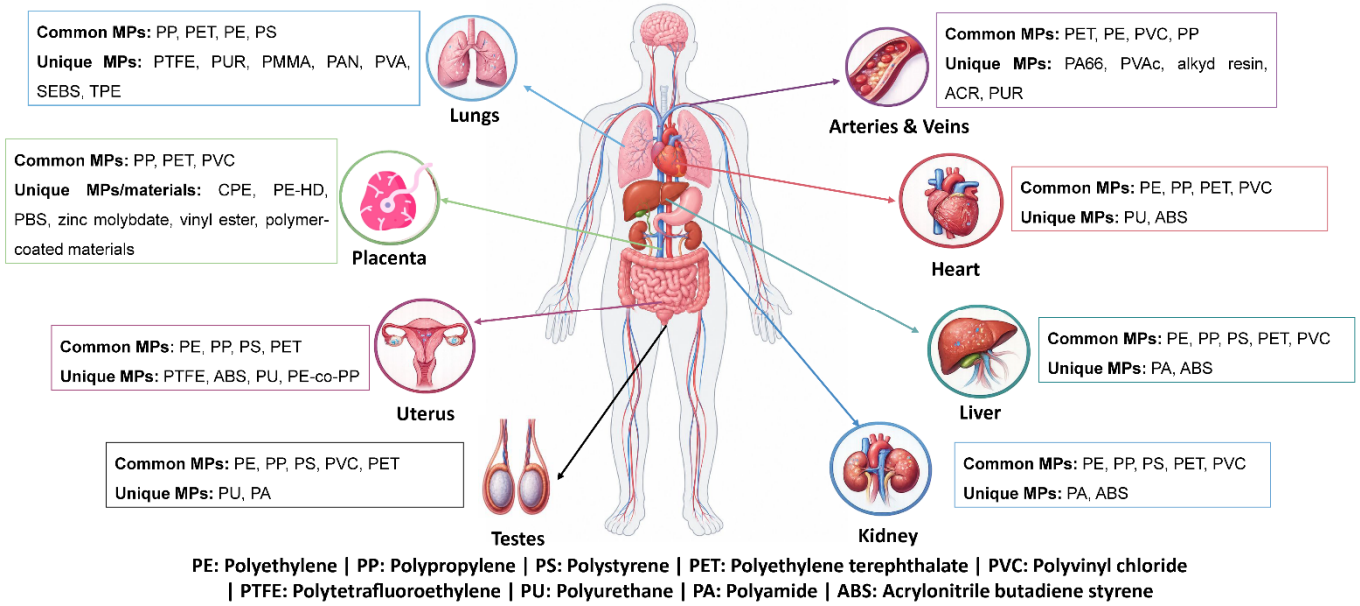


Figure 3. Distribution of MPs in Human Tissues and Organs.

5. Potential Human Health Implications of MPs

The widespread detection of MPs in human tissues, body fluids, and excreta has raised growing concerns regarding their potential implications for human health. Although direct causal evidence in humans remains limited, accumulating findings from observational studies, in vitro investigations, and evidence derived from environmental and animal models suggest several plausible biological mechanisms through which MPs may contribute to adverse health outcomes. Before causing toxic effects in different organs, MPs and NPs that enter the bloodstream quickly interact with biological fluids. Their surfaces adsorb plasma proteins such as albumin, fibrinogen, apolipoproteins, and immunoglobulins, forming a protein corona. This protein corona changes the biological identity of the particles and influences their biodistribution, cellular uptake, and interactions with immune cells. It may also affect their circulation time and influence their interactions with biological barriers, including the placenta and the blood–brain barrier [105–108]. As a result, MPs and NPs can reach different organs and contribute to the toxic effects discussed in the following sections.

5.1. Reproductive System

Several studies have raised concerns regarding the potential effects of MPs on both male and female reproductive health. In males, growing evidence suggests that MP exposure may adversely influence reproductive function. For example, Zhao et al. reported

that MP contamination in the male reproductive system may be associated with reduced sperm concentration and motility [11]. Similarly, Guo et al. proposed that MP exposure could impair semen quality while also contributing to decreased testosterone levels [44]. Supporting these observations, Montano et al. identified MPs directly within human semen samples and highlighted that particles measuring as small as 2–6 μm may interfere with normal sperm function [15]. Together, these findings suggest that MPs may have the potential to compromise male reproductive health through multiple biological pathways.

Concerns have also emerged regarding the impact of MPs on female reproductive health. Due to their small size (<100 μm), MPs may penetrate cellular barriers and trigger oxidative stress, inflammatory responses, and DNA damage within endometrial tissues [36]. Beyond direct cellular effects, MPs may also contribute to hormone-related reproductive disorders. Xu et al. suggested that MPs could promote fibroid development by adsorbing environmental estrogens or inducing endocrine-disrupting effects [33]. Further mechanistic evidence was provided by Kim et al., who demonstrated that polystyrene nanoparticles can induce apoptosis in endometrial stromal cells, indicating a possible link between plastic exposure and reproductive tissue damage [92]. Although this study provides important mechanistic insights, it was conducted using engineered polystyrene NPs, and therefore its findings should be interpreted specifically in the context of NPs. Clinical observations further strengthen these concerns. Peng et al. reported significantly higher MP concentrations in diseased uterine tissues, including fibroids, endometrial cancer, and cervical cancer, compared with healthy tissues, suggesting a potential association between MP accumulation and gynecological disorders [13]. Likewise, Dong et al. identified MPs in adenomyosis lesions, ovarian ectopic cysts, and uterine tubes, highlighting the widespread distribution of MPs throughout the female reproductive tract [27]. Moreover, evidence of MP presence in the placenta has raised concerns regarding maternal and fetal health. Ragusa et al. proposed that placental MPs may alter immune regulation at the maternal–fetal interface and potentially contribute to metabolic abnormalities during pregnancy [29]. Thus, these findings suggest that MP exposure may influence reproductive health through multiple mechanisms, although further research is needed to clarify causal relationships and long-term consequences.

5.2. Cardiovascular System

The detection of MPs in blood, thrombi, and vascular tissues has raised increasing concerns regarding their potential implications for cardiovascular health. Emerging evidence suggests that MPs may influence multiple biological processes involved in vascular function, inflammation, and thrombotic events. Leonard et al. highlighted that nanoparticles can alter platelet aggregation and thrombus formation, indicating that MPs may be associated with a pro-thrombotic state or an increased susceptibility to bleeding disorders [43]. Supporting this concern, Wu et al. proposed that elevated MP concentrations in the bloodstream could increase interactions among platelets and early thrombi, potentially accelerating thrombosis. They further suggested that the cardiovascular risks associated with MP exposure may currently be underestimated, particularly in conditions such as ischaemic heart disease and stroke [60].

Beyond thrombosis-related mechanisms, MPs may also play a role in vascular pathology. Liu et al. observed significantly higher MP concentrations in arteries containing atherosclerotic plaques compared with the aorta. However, this finding should be interpreted with caution, as the higher abundance of MPs in atherosclerotic lesions may reflect either a potential involvement of MPs in vascular pathology or the preferential retention of circulating MPs within diseased vessels due to lesion-associated alterations in vascular structure, inflammation, and microcirculation [39]. Similar concerns have been reported

in cerebrovascular disease. Wang et al. found that patients with ischaemic stroke who exhibited higher MP concentrations tended to experience more severe clinical outcomes, proposing that MPs may accumulate within the circulatory system and contribute to thrombus formation or stability [62]. Together, these findings suggest an association between MPs and cardiovascular disease, and several biologically plausible mechanisms have been proposed involving thrombosis, vascular injury, and circulatory disturbances. However, whether MPs contribute to these pathological processes or preferentially accumulate within pre-existing vascular lesions remains uncertain. Additional evidence indicates that MP exposure may also occur through medical interventions and environmental sources encountered during healthcare procedures. Yang et al. suggested that invasive procedures, including cardiac surgery, may facilitate the direct introduction of MPs into the bloodstream and surrounding tissues. They further noted that polyvinyl chloride (PVC) particles have been associated with pro-inflammatory responses in adipocytes, while polycarbonate (PC) particles are recognised endocrine disruptors. Importantly, the detection of MPs within the myocardium and pericardium suggests that MP contamination may extend to deep cardiovascular anatomical structures [50]. Similarly, Rotchell et al. proposed that MPs present in vascular tissues may contribute to inflammatory disorders and adverse cardiovascular outcomes. They additionally highlighted that patients undergoing surgery may experience exposure to MPs originating from synthetic paints, varnishes, and plastic materials commonly present within operating room environments [32]. Therefore, current evidence supports an association between MPs and cardiovascular dysfunction, and several biologically plausible mechanisms have been proposed, including inflammation, thrombosis, vascular injury, and environmental or procedural exposure routes. However, current human studies remain largely observational, and it is unclear whether MPs contribute to cardiovascular disease or preferentially accumulate within pre-existing vascular lesions. Further mechanistic and longitudinal studies are needed to clarify the direction of this association.

5.3. Respiratory System

The respiratory tract represents one of the primary pathways through which humans may be exposed to MPs, particularly through inhalation of airborne particles. Growing evidence suggests that inhaled MPs may accumulate within respiratory tissues and potentially contribute to adverse pulmonary effects. Huang et al. confirmed that MPs present in environmental dust can be inhaled and retained within the trachea and lungs. They further observed that individuals with occupational exposure to elevated MP concentrations may experience a higher prevalence of respiratory symptoms, including coughing, dyspnoea, and wheezing [54]. These findings raise concerns regarding the long-term consequences of chronic MPs inhalation, particularly among highly exposed populations. Potential biological mechanisms underlying respiratory effects have also been proposed. Jenner et al. highlighted that MPs deposited in lung tissues may promote inflammation, reactive oxygen species (ROS) generation, and physical tissue damage. In addition, MPs may act as carriers of chemical additives or adsorbed environmental pollutants, potentially amplifying their harmful effects within the respiratory system [31]. Supporting these concerns, Tokito et al. suggested that airborne MPs may contribute to lung inflammation in a manner comparable to particulate matter (PM_{10}), indicating that MPs could represent an additional environmental factor influencing respiratory health [7]. Clinical observations further strengthen the growing concern regarding pulmonary exposure to MPs. Özgen Alpaydin et al. detected MPs in bronchoalveolar lavage fluid obtained from patients with interstitial lung disease and proposed that MP exposure may contribute to disease development or progression [30]. Collectively, these findings suggest that inhaled MPs may influence respiratory health

through multiple pathways, including particle retention, oxidative stress, inflammation, and pollutant transport. However, further studies are required to better understand the long-term health implications and establish causal relationships between MP exposure and respiratory disease outcomes.

5.4. Gastrointestinal and Hepatobiliary Systems

The gastrointestinal tract is a major route of MP exposure through the ingestion of contaminated food, water, and environmental dust. Emerging evidence suggests that ingested MPs may cross the gastrointestinal barrier, enter the bloodstream, and reach distant organs, providing a plausible route for systemic distribution [25]. Song et al. further highlighted concerns that MPs may cause physical tissue damage or act as carriers of endocrine-disrupting chemicals and other contaminants [46]. Recent findings also suggest potential effects of MPs on hepatobiliary health. Zhang et al. proposed that younger individuals may be more susceptible to MPs-related gallstone formation due to greater consumption of food and beverages packaged in plastic materials [55]. Similarly, Wang et al. suggested that MPs may contribute to both biliary inflammation and gallstone development [35]. In addition, Horvatits et al. proposed that chronic liver disease and increased intestinal permeability may facilitate MP accumulation within liver tissues [14]. Özsoy et al. further suggested that smaller MP particles generated during degradation may pass through the digestive system more easily and potentially contribute to cytotoxic, genotoxic, and metabolic disturbances [47]. Taken together, the available evidence suggests that MPs may influence gastrointestinal and hepatobiliary health through multiple biological pathways, including physical tissue interaction, chemical additive transport, and inflammatory responses. Unlike other organ systems, the gastrointestinal tract represents both the primary portal of MP exposure and a potential site of absorption, degradation, and redistribution. Consequently, distinguishing between transient passage and biologically significant tissue accumulation remains challenging. Current evidence supports the presence of MPs within gastrointestinal and hepatobiliary tissues; however, it remains unclear whether these particles directly contribute to disease pathogenesis or accumulate as a consequence of pre-existing pathological conditions.

5.5. Urinary System

Recent studies have demonstrated that MPs can accumulate within different parts of the human urinary system, including urine and kidney tissues. Evidence suggests that MPs entering the body through ingestion or inhalation may eventually be transported to the kidneys and eliminated through urinary excretion. In this context, Pironti et al. proposed that MPs can move through the gastrointestinal tract and later reach the urinary system for excretion. Interestingly, they observed that the detected particles (4–15 μm) were larger than the size typically allowed to cross the glomerular filtration barrier, suggesting that these MPs may instead pass through the renal tubular system [64]. Supporting this observation, Massardo et al. further confirmed the presence of MPs in both kidney tissue and urine samples, providing additional evidence that MPs are capable of reaching and persisting within the human urinary system [51].

5.6. Ocular System

The detection of MPs in ocular components such as the vitreous humour, aqueous humour, tear fluid, and meibum has raised growing concerns regarding their potential impact on eye health. Recent studies suggest that MPs may not only reach ocular tissues but may also interfere with normal ocular physiology through multiple biological mechanisms. For instance, Zong et al. identified MPs in vitreous humour and proposed that the blood–retinal barrier may not provide complete protection against MP translocation into

ocular tissues [45]. Similarly, Zhang et al. suggested that MPs may cross the blood–aqueous barrier, allowing particles circulating in the bloodstream to enter the eye, which could negatively influence ocular health [87]. In addition to their presence within ocular compartments, Wang et al. highlighted several possible mechanisms through which MPs may contribute to ocular damage, including direct cellular toxicity, oxidative stress induction, and inflammatory responses on the ocular surface [58].

5.7. Musculoskeletal and Other Systems

Emerging evidence suggests that MPs may also accumulate in musculoskeletal and other body systems, raising concerns regarding their potential biological effects. Li et al. detected MPs in synovial tissues of hip and knee joints and suggested that their presence may contribute to local inflammatory responses, although the underlying mechanisms remain unclear [53]. Similarly, Guo et al. highlighted that the detection of MPs in bone marrow indicates deeply embedded exposure, with smaller particles (<100 μm) potentially having greater mobility and biological impact [57]. Potential concerns have also been reported in developmental and other physiological systems. Zhang et al. identified MPs in meconium and infant stool, suggesting possible early-life exposure and raising concerns regarding fetal development [48]. In addition, Saraluck et al. proposed that MPs present in human breast milk may alter microbial balance by influencing bacterial growth patterns, potentially contributing to dysbiosis [28]. MPs have also been detected in reproductive-associated tissues beyond the female reproductive tract. Demirelli et al. (2024) suggested that MPs identified in the prostate may have implications for prostatic health, although further mechanistic studies are required [10]. Similarly, Codrington et al. proposed that MP accumulation in penile tissue could potentially influence erectile function through vascular-related mechanisms [9]. Overall, these findings suggest that MP exposure may extend beyond traditionally studied organ systems, highlighting the widespread distribution of MPs within the human body and the need for further investigation into their long-term biological consequences.

5.8. Cancer and Tumor Progression

The detection of MPs in multiple tumor tissues has generated increasing interest regarding their possible involvement in cancer biology. MPs have been identified in several cancer types, including cervical, lung, gastric, colorectal, pancreatic, renal, prostate, and penile cancers, highlighting their widespread distribution in diseased tissues. Xu et al. suggested that MPs may penetrate the gastrointestinal barrier, enter circulation, and accumulate in distant organs, where they may interact with the tumor microenvironment [25]. Likewise, Zhao et al. identified MPs across various tumor types and emphasised the need for further investigation into their potential role in carcinogenesis [12]. Several biological mechanisms have been proposed to explain how MPs could influence tumor-related processes. Deng et al. suggested that MPs may promote oxidative stress and inflammation while also serving as carriers of toxic compounds, pathways that are commonly associated with cancer progression [63]. Supporting these observations, Zhang et al. reported significantly greater accumulation of MPs in renal carcinoma tissues than in adjacent healthy tissues. These findings have led to two competing hypotheses regarding the relationship between MPs and cancer. The first hypothesis proposes that chronic exposure to MPs may contribute to carcinogenesis or tumor progression through biologically plausible mechanisms, including oxidative stress, persistent inflammation, genotoxicity, endocrine disruption, and the transport of adsorbed environmental contaminants. In contrast, the second hypothesis suggests that MPs do not actively promote tumor development but instead accumulate passively within established tumors because malignant tissues often

exhibit enhanced vascular permeability, disrupted tissue architecture, altered microcirculation, and impaired lymphatic drainage, which may facilitate the retention of circulating particles [38]. Current human evidence is insufficient to distinguish between these hypotheses, as available studies are primarily cross-sectional and observational. Despite these observations, current evidence remains primarily correlational, and none of the available studies have established a direct causal relationship between MP exposure and cancer development. Further mechanistic investigations and well-designed longitudinal cohort studies are therefore required to distinguish between these competing hypotheses and clarify the direction of this association.

Across the available literature, several interconnected biological mechanisms have been proposed to explain how MPs may influence human health, including oxidative stress, inflammatory responses, DNA damage, endocrine disruption, physical tissue injury, and the release of chemical additives and adsorbed environmental contaminants. Beyond the physical effects of plastic particles, chemical additives released from MPs and NPs, such as plasticizers, stabilizers, and flame retardants, may also contribute to toxicity. These chemicals can disrupt endocrine signaling, increase oxidative stress, and trigger inflammatory responses, which may further damage different tissues and organs [109–111]. Similarly, MPs can also adsorb environmental contaminants, including heavy metals, persistent organic pollutants, and per- and polyfluoroalkyl substances, potentially acting as carriers of these chemicals and thereby enhancing their toxic effects [112]. However, most current human biomonitoring studies primarily focus on polymer identification and particle characteristics, whereas the chemical additives and adsorbed contaminants associated with MPs in human tissues remain largely uncharacterized [20]. Future studies integrating polymer identification with the characterization of chemical additives and adsorbed contaminants are therefore needed to better elucidate the contribution of these co-occurring chemicals to MP-associated toxicity. Moreover, once MPs and NPs enter the bloodstream, they may rapidly adsorb plasma proteins to form a protein corona, which alters their biological identity and may influence biodistribution, cellular uptake, immune recognition, prolonged circulation, and interactions with biological barriers such as the placenta and blood–brain barrier [105,108]. The small size of many detected particles, frequently measuring below 10 μm and in some cases as small as 1–5 μm, may facilitate cellular internalisation, movement across biological barriers, and accumulation within deep tissues and organs. The widespread detection of MPs across diverse human tissues and body fluids, together with these biologically plausible mechanisms, highlights the growing importance of understanding their long-term health implications. Although these proposed mechanisms are biologically plausible, current human evidence remains largely associative and does not establish a causal relationship between MP exposure and cancer or other pathological conditions. Consequently, it remains unresolved whether MPs contribute to disease initiation and progression or preferentially accumulate in diseased tissues because of pathological alterations in tissue structure and vascular permeability. The consistent presence of MPs in the human body underscores the urgent need for standardised detection methodologies, longitudinal investigations, and comprehensive risk assessment frameworks to better evaluate the consequences of chronic environmental exposure to MPs and to guide future public health strategies.

Taken together, the organ-specific evidence discussed above indicates that the adverse health effects of MPs are mediated through several interconnected biological processes rather than entirely distinct organ-specific pathways. As summarized in Figure 4, following cellular uptake, MPs can initiate physical injury, oxidative stress, inflammatory responses, endocrine disruption, and vector-mediated toxicity, which together contribute to cellular dysfunction and subsequent tissue injury in multiple organs. Although the pathological

manifestations differ according to the physiological characteristics and functions of individual organs, the available evidence indicates that these common mechanisms appear to collectively underlie the diverse health outcomes associated with MP exposure. Therefore, integrating organ-specific findings within a unified mechanistic framework provides a more comprehensive understanding of MP toxicity and highlights that many reported adverse effects arise from shared toxicological pathways rather than isolated organ-specific mechanisms. Although comparing MP concentrations detected in human tissues with the effect doses reported in toxicological studies would be valuable for risk assessment, such comparisons remain challenging. Human biomonitoring studies quantify MPs using heterogeneous metrics (e.g., particles/mL, particles/g, or mass concentration) and employ different analytical methods with varying detection limits. In contrast, experimental toxicological studies typically use controlled exposure doses (e.g., mg/kg, μg/mL, or particle numbers) under in vitro or animal models that are not directly comparable with measured human body burdens. Consequently, current evidence does not permit a reliable quantitative dose–response assessment or direct comparison between human exposure levels and experimentally derived effect doses, highlighting the need for standardized exposure metrics and environmentally relevant experimental designs to strengthen future human health risk assessment.

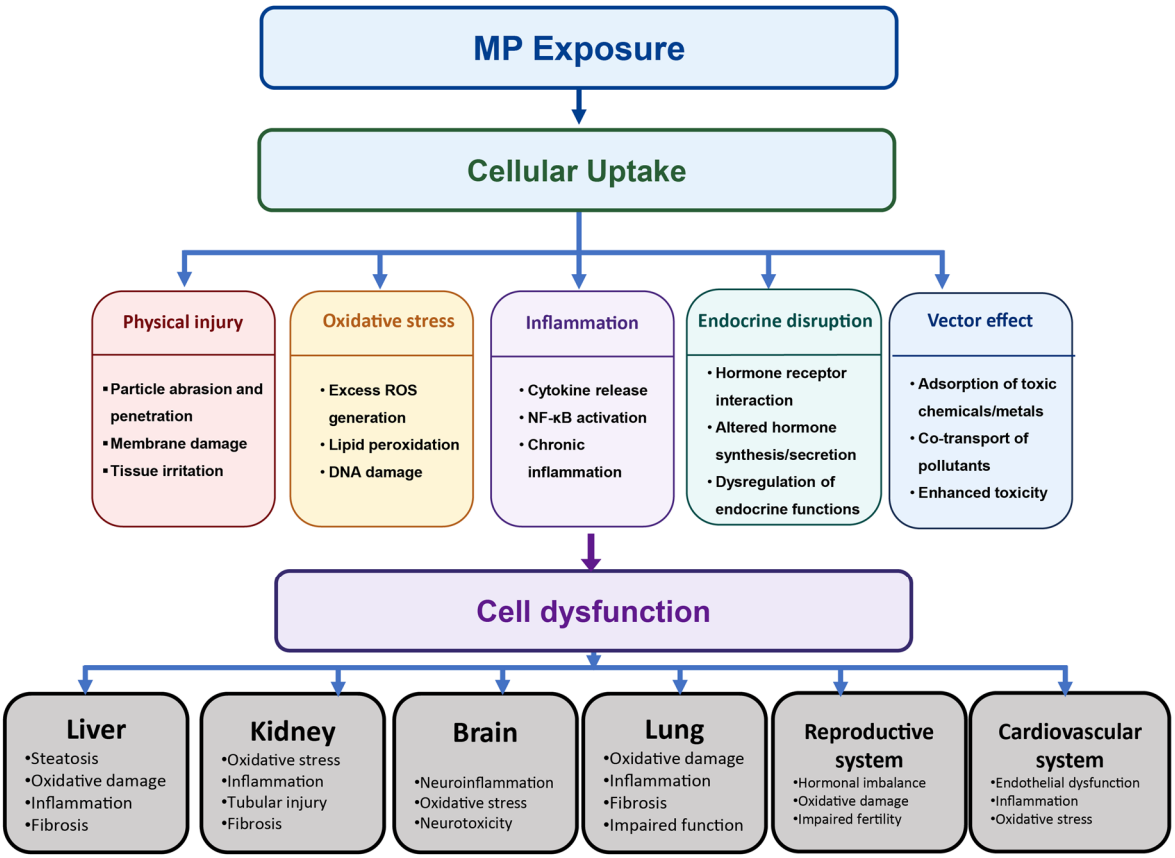


Figure 4. Unified mechanistic framework illustrating the common toxicological pathways underlying microplastic-induced organ toxicity.

6. Limitations

This narrative review has several limitations that should be considered when interpreting the findings. First, the studies included in this review employed different sample preparation methods, detection techniques, and reporting approaches. These methodological differences may have influenced the reported abundance, size, and polymer composition

of MPs, making direct comparisons between studies difficult. Second, the analytical methods used across studies, such as Raman spectroscopy, μ-FTIR, LDIR, and Py-GC/MS, differ in their sensitivity and detection limits, which may contribute to variations in reported findings. In addition, many studies were conducted with relatively small sample sizes and focused on specific populations or geographic regions. As a result, the findings may not fully represent the broader human population. Furthermore, most of the available evidence is derived from observational, predominantly cross-sectional studies, which preclude causal inference between MP exposure and adverse health outcomes. Although several studies have reported higher MP abundance in tumor tissues, vascular lesions, and other diseased organs than in corresponding control tissues, these observations should not be interpreted as evidence of a causal relationship. It remains unclear whether MPs contribute to the development or progression of these pathological conditions or whether disease-associated alterations in tissue architecture, vascular permeability, inflammation, or microcirculation promote the preferential retention and accumulation of MPs. Therefore, the direction of this association cannot currently be established. In addition, many human studies did not adequately control for potential confounding factors, such as diet, occupation, lifestyle, and environmental exposure, which may have influenced the reported associations between MP exposure and tissue accumulation. Moreover, establishing a quantitative dose–response relationship remains challenging because human biomonitoring studies report MP abundance using heterogeneous metrics (e.g., particle counts or mass concentrations), whereas toxicological studies often employ different exposure units, experimental conditions, and substantially higher doses. Consequently, direct comparisons between MP concentrations detected in human tissues and the effect doses reported in experimental studies are currently not feasible, limiting realistic human health risk assessment. Future studies should adopt standardized exposure metrics and environmentally relevant dose ranges to facilitate quantitative risk assessment and improve the translation of experimental findings to human health. Although MPs have been detected in a wide range of human tissues and biological fluids, their long-term health effects, biological fate, and clearance mechanisms remain poorly understood. Finally, the lack of standardized protocols for the detection and characterization of MPs continues to limit the comparability and reproducibility of existing studies. Future research should focus on developing standardized methodologies and conducting large-scale, longitudinal, and mechanistic studies to better understand human exposure, clarify causal relationships, and determine the biological and clinical implications of MP accumulation in the human body.

7. Conclusions

This review consolidates current evidence on the occurrence of microplastics across human organs, tissues, and biological fluids while providing a comparative assessment of the analytical methodologies used for their detection. By synthesizing these diverse areas within a single framework, it highlights overall distribution patterns, methodological heterogeneity, and key knowledge gaps that are difficult to identify from individual studies alone. Collectively, the evidence synthesized in this review demonstrates that MPs have now been detected in a wide range of human tissues, organs, and biological fluids, including blood, placental tissues, reproductive tissues, breast milk, urine, stool, respiratory samples, and cardiovascular tissues, highlighting the widespread nature of human exposure. Across the narrative reviewed studies, PE, PP, PS, PET, and PVC were the most frequently identified polymer types. Advances in analytical techniques, including Raman spectroscopy, μ-FTIR, LDIR, and Py-GC/MS, have greatly improved the detection and characterization of MPs in complex biological matrices, providing valuable insights into their occurrence and distribution within the human body. This comparative evaluation

further illustrates how methodological differences contribute to the variability observed in reported microplastic abundance, size distributions, and polymer composition across human studies. Nevertheless, substantial variability in sampling strategies, contamination control procedures, particle identification criteria, and analytical methodologies continues to hamper direct comparisons among studies, emphasizing the need for standardized protocols and reporting practices. Furthermore, although this review primarily focuses on microplastics, current analytical techniques have limited sensitivity for detecting nanoplastics and the smallest microplastic fractions. Consequently, the reported occurrence and distribution of plastic particles in human tissues may underestimate the actual internal burden, thereby limiting our current understanding of their distribution, biological fate, and potential health effects. Although a growing body of evidence suggests potential associations between MP exposure and adverse biological effects, such as inflammation, oxidative stress, endocrine disruption, and tissue damage, current findings remain insufficient to establish clear causal relationships with specific human diseases. Future research should therefore prioritize the development of standardized and validated protocols for detecting and quantifying NPs in human biological samples, elucidating in vivo mechanisms governing MP and NP translocation across biological barriers, and establishing large prospective birth cohort studies to evaluate the long-term health consequences of prenatal and early-life exposure. In addition, harmonized analytical approaches, mechanistic toxicological studies, and large-scale epidemiological investigations are needed to better understand the sources, fate, biological behavior, and health implications of MPs in humans. Overall, this review provides a consolidated framework for understanding the occurrence, detection methodologies, and body-wide distribution of microplastics in humans while identifying the major methodological limitations and research priorities that should guide future investigations. The available evidence also highlights MPs as an emerging public health concern and emphasizes the importance of continued multidisciplinary research and robust risk assessment frameworks to clarify their long-term consequences for human health.

Supplementary Materials: The following supporting information can be downloaded at: https://www.mdpi.com/article/10.3390/microplastics5030157/s1, Table S1. Head-to-head comparison of the major analytical techniques used for microplastic detection and characterization in human biological samples; Table S2. Statistical summary of microplastic occurrence and characteristics in human biological fluids based on the studies included in Table 3; Table S3. Statistical summary of the occurrence, concentration, predominant polymer types, and particle size characteristics of microplastics in human tissues and organs across the studies summarized in Table 4.

Author Contributions: H.S.: Formal analysis, Investigation, Methodology, Visualization, Software, Writing—original draft, Writing—narrative review and editing; U.H.M.: Writing—original draft, Writing—narrative review and editing; G.S.: Conceptualization, Supervision, Data curation, Formal analysis, Investigation, Writing—original draft, Writing—narrative review and editing; A.B.: Data curation, Writing—original draft, Writing—narrative review and editing; B.M.R.H.: Writing—narrative review and editing. All authors have read and agreed to the published version of the manuscript.

Funding: This study received no external funding.

Data Availability Statement: No new data were created or analyzed in this study. Data sharing is not applicable to this article.

Acknowledgments: Generative artificial intelligence (AI) tools, specifically ChatGPT (GPT-5 model), were used in this study to assist with language refinement, grammar checking, and improving the clarity and flow of the manuscript.

Conflicts of Interest: The authors declare no conflicts of interest.

Abbreviations

The following abbreviations are used in this manuscript:

MP	Microplastic
MPs	Microplastics
NPs	Nanoplastics
PE	Polyethylene
PP	Polypropylene
PET	Polyethylene terephthalate
PS	Polystyrene
PVC	Polyvinyl chloride
PA	Polyamide
PA66	Polyamide 66
PC	Polycarbonate
PMMA	Poly(methyl methacrylate)
PAN	Polyacrylonitrile
PU	Polyurethane
PVA	Poly(vinyl alcohol)
PES	Polyethersulfone
HDPE	High-density polyethylene
SEBS	Styrene–ethylene–butylene–styrene
TPE	Thermoplastic elastomer
CPE	Chlorinated polyethylene
μ-FTIR	Micro-Fourier transform infrared spectroscopy
ATR-FTIR	Attenuated total reflectance Fourier transform infrared spectroscopy
LDIR	Laser direct infrared imaging
Py-GC/MS	Pyrolysis–gas chromatography/mass spectrometry
RMS	Raman microscopy
μ-Raman	Micro-Raman spectroscopy
SEM	Scanning electron microscopy
SEM-EDX	Scanning electron microscopy–energy-dispersive X-ray spectroscopy
LC-MS/MS	Liquid chromatography–tandem mass spectrometry
QCL	Quantum cascade laser
ROS	Reactive oxygen species
RNA-seq	RNA sequencing
BKMR	Bayesian kernel machine regression
LOD	Limit of detection
LOQ	Limit of quantification
BAL	Bronchoalveolar lavage
BALF	Bronchoalveolar lavage fluid
PTFE	Polytetrafluoroethylene
KOH	Potassium hydroxide
H_2O_2	Hydrogen peroxide
HNO_3	Nitric acid
NaOH	Sodium hydroxide
NaClO	Sodium hypochlorite
SDS	Sodium dodecyl sulfate
Tris-HCl	Tris(hydroxymethyl)aminomethane hydrochloride
$CaCl_2$	Calcium chloride

References

1. Li, Y.; Chen, L.; Zhou, N.; Chen, Y.; Ling, Z.; Xiang, E.P. Microplastics in the human body: A comprehensive review of exposure, distribution, migration mechanisms, and toxicity. *Sci. Total Environ.* **2024**, *946*, 174215. [CrossRef] [PubMed]
2. Schmid, C.; Cozzarini, L.; Zambello, E.E. Microplastic's story. *Mar. Pollut. Bull.* **2021**, *162*, 111820. [CrossRef] [PubMed]

3. Subhamgi, T.B.; Jayanarayanan, B.; Thomas, J.; Lakshmi Ammal, E.P.K. Mapping Scientific Research on Microplastics in Wetland Ecosystems in South Asia and Southeast Asia: Bibliometric Insights on Remediation Technologies, Including Nanoremediation. *Earth* **2026**, *7*, 69. [CrossRef]
4. Li, D.; Li, P.; Shi, Y.; Sheerin, E.D.; Zhang, Z.; Yang, L.; Xiao, L.; Hill, C.; Gordon, C.; Ruether, M.; et al. Stress-induced phase separation in plastics drives the release of amorphous polymer micropollutants into water. *Nat. Commun.* **2025**, *16*, 3814. [CrossRef] [PubMed]
5. Sarker, H.; Saha, G.; Bhowmik, A.; Ganguly, E.A. Microplastics as Emerging One Health Threats: A Molecular and Ecotoxicological Review Across Aquatic Life with Emphasis on Fish. *Microplastics* **2026**, *5*, 102. [CrossRef]
6. PlasticsEurope. Plastics—The Fast Facts 2025: An Analysis of European Plastics Production, Demand and Waste Data. 2025. Available online: https://plasticseurope.org/knowledge-hub/plastics-the-fast-facts-2025/ (accessed on 15 April 2026).
7. Tokito, T.; Kido, T.; Nagafuchi, O.; Tomoshige, K.; Nakazawa, K.; Shinozuka, K.; Sato, S.; Kido, K.; Noguchi, Y.; Matsumoto, T.; et al. Microplastics in Human Bronchoalveolar Lavage Fluid. *Respirology* **2025**, *30*, 1141–1152. [CrossRef] [PubMed]
8. Tian, J.; Liang, L.; Li, Q.; Li, N.; Zhu, X.; Zhang, E.L. Association between microplastics in human amniotic fluid and pregnancy outcomes: Detection and characterization using Raman spectroscopy and pyrolysis GC/MS. *J. Hazard. Mater.* **2025**, *482*, 136637. [CrossRef] [PubMed]
9. Codrington, J.; Varnum, A.A.; Hildebrandt, L.; Pröfrock, D.; Bidhan, J.; Khodamoradi, K.; Höhme, A.-L.; Held, M.; Evans, A.; Velasquez, D.; et al. Detection of microplastics in the human penis. *Int. J. Impot. Res.* **2025**, *37*, 377–383. [CrossRef] [PubMed]
10. Demirelli, E.; Tepe, Y.; Oğuz, U.; Aydın, H.; Kodat, M.; Tok, D.S.; Sönmez, M.G.; Öğreden, E. The first reported values of microplastics in prostate. *BMC Urol.* **2024**, *24*, 106. [CrossRef] [PubMed]
11. Zhao, Q.; Zhu, L.; Weng, J.; Jin, Z.; Cao, Y.; Jiang, H.; Zhang, Z. Detection and characterization of microplastics in the human testis and semen. *Sci. Total Environ.* **2023**, *877*, 162713. [CrossRef] [PubMed]
12. Zhao, J.; Zhang, H.; Shi, L.; Jia, Y.; Sheng, E.H. Detection and quantification of microplastics in various types of human tumor tissues. *Ecotoxicol. Environ. Saf.* **2024**, *283*, 116818. [CrossRef] [PubMed]
13. Peng, J.; Lin, Y.; Yao, F.; Ma, D.; Yu, J.; Dong, E.C. Raman-based profiling of microplastics in human uterine tissue: A new dimension in reproductive toxicology. *J. Environ. Chem. Eng.* **2026**, *14*, 121418. [CrossRef]
14. Horvatits, T.; Tamminga, M.; Liu, B.; Sebode, M.; Carambia, A.; Fischer, L.; Püschel, K.; Huber, S.; Fischer, E.K. Microplastics detected in cirrhotic liver tissue. *eBioMedicine* **2022**, *82*, 104147. [CrossRef] [PubMed]
15. Montano, L.; Giorgini, E.; Notarstefano, V.; Notari, T.; Ricciardi, M.; Piscopo, M.; Motta, O. Raman Microspectroscopy evidence of microplastics in human semen. *Sci. Total Environ.* **2023**, *901*, 165922. [CrossRef] [PubMed]
16. Nawab, A.; Ahmad, M.; Khan, M.T.; Nafees, M.; Khan, I.; Ihsanullah, E.I. Human exposure to microplastics: A review on exposure routes and public health impacts. *J. Hazard. Mater. Adv.* **2024**, *16*, 100487. [CrossRef]
17. Bai, C.-L.; Wang, D.; Luan, Y.-L.; Huang, S.-N.; Liu, L.-Y.; Guo, E.Y. A review on micro- and nanoplastics in humans: Implication for their translocation of barriers and potential health effects. *Chemosphere* **2024**, *361*, 142424. [CrossRef] [PubMed]
18. Dmitrowicz, A.; Sacharczuk, M.; Skiba, E.D. Micro- and nanoplastics in human biological materials: A systematic review of detection methods and methodological challenges. *Arch. Toxicol.* **2026**, *100*, 3841–3855. [CrossRef] [PubMed]
19. Huang, Z.; Hu, B.; Wang, E.H. Analytical methods for microplastics in the environment: A review. *Environ. Chem. Lett.* **2023**, *21*, 383–401. [CrossRef] [PubMed]
20. Roslan, N.S.; Lee, Y.Y.; Ibrahim, Y.S.; Anuar, S.T.; Yusof, K.M.K.K.; Lai, L.A.; Brentnall, T. Detection of microplastics in human tissues and organs: A scoping review. *J. Glob. Health* **2024**, *14*, 04179. [CrossRef] [PubMed]
21. Doroftei, B.; Savuca, A.; Cretu, A.-M.; Maftei, R.; Anton, N.; Ilea, C.; Doroftei, M.; Puha, B. Microplastics and human fertility: A comprehensive review of their presence in human samples and reproductive implication. *Ecotoxicol. Environ. Saf.* **2025**, *303*, 118939. [CrossRef] [PubMed]
22. Lee, D.-W.; Jung, J.; Park, S.-A.; Lee, Y.; Kim, J.; Han, C.; Kim, H.-C.; Lee, J.H.; Hong, Y.-C. Microplastic particles in human blood and their association with coagulation markers. *Sci. Rep.* **2024**, *14*, 30419. [CrossRef] [PubMed]
23. Sunil, M.; Mithun, N.; Xavier, K.A.M.; Nayak, G.; Kalthur, G.; Chidangil, S.; Kumar, S.; Lukose, J. Exploring the detrimental effects of nanoplastics on ecosystems and human health. *J. Hazard. Mater. Adv.* **2025**, *19*, 100831. [CrossRef]
24. Xu, H.; Yu, Z.; Xie, Y. Quantitative human biomonitoring of micro- and nanoplastics: Exposure profiles, mechanistic insights, and health implications. *J. Hazard. Mater.* **2026**, *502*, 141054. [CrossRef] [PubMed]
25. Xu, H.; Dong, C.; Yu, Z.; Ozaki, Y.; Hu, Z.; Zhang, B.; Yao, W.; Yu, J.; Xie, Y. Detection and analysis of microplastics in tissues and blood of human cervical cancer patients. *Environ. Res.* **2024**, *259*, 119498. [CrossRef] [PubMed]
26. Wang, C.; Chang, H.; Wang, H.; Li, H.; Ding, S.; Ren, E.F. Exposure to microplastics during pregnancy and fetal liver function. *Ecotoxicol. Environ. Saf.* **2025**, *294*, 118099. [CrossRef] [PubMed]
27. Dong, C.; Xu, H.; Lin, Y.; Zhang, B.; Yu, Z.; Xie, Y.; Yu, J.; Ma, D. Microplastics detected in three types of female reproductive organs using micro-Raman spectroscopy. *Ecotoxicol. Environ. Saf.* **2024**, *285*, 117099. [CrossRef] [PubMed]

28. Saraluck, A.; Techarang, T.; Bunyapipat, P.; Boonchuwong, K.; Pullaput, Y.; Mordmuang, E.A. Detection of Microplastics in Human Breast Milk and Its Association with Changes in Human Milk Bacterial Microbiota. *J. Clin. Med.* **2024**, *13*, 4029. [CrossRef] [PubMed]
29. Ragusa, A.; Svelato, A.; Santacroce, C.; Catalano, P.; Notarstefano, V.; Carnevali, O.; Papa, F.; Rongioletti, M.C.A.; Baiocco, F.; Draghi, S.; et al. Plasticenta: First evidence of microplastics in human placenta. *Environ. Int.* **2021**, *146*, 106274. [CrossRef] [PubMed]
30. Alpaydin, A.Ö.; Uçan, E.S.; Köktürk, M.; Atamanalp, M.; Kalyoncu, Ç.; Yiğit, S.; Uçar, A.; Şimşek, G.Ö.; Tertemiz, K.C.; Karaçam, V.; et al. Microplastics, as a risk factor in the development of interstitial lung disease- a preliminary study. *Environ. Pollut.* **2024**, *363*, 125054. [CrossRef] [PubMed]
31. Jenner, L.C.; Rotchell, J.M.; Bennett, R.T.; Cowen, M.; Tentzeris, V.; Sadofsky, E.L.R. Detection of microplastics in human lung tissue using μFTIR spectroscopy. *Sci. Total Environ.* **2022**, *831*, 154907. [CrossRef] [PubMed]
32. Rotchell, J.M.; Jenner, L.C.; Chapman, E.; Bennett, R.T.; Bolanle, I.O.; Loubani, M.; Sadofsky, L.; Hobkirk, J.; Palmer, T.M. Detection of microplastics in human saphenous vein tissue using μFTIR: A pilot study. *PLoS ONE* **2023**, *18*, e0280594. [CrossRef] [PubMed]
33. Xu, H.; Dong, C.; Yu, Z.; Hu, Z.; Yu, J.; Ma, D.; Yao, W.; Qi, X.; Ozaki, Y.; Xie, Y. First identification of microplastics in human uterine fibroids and myometrium. *Environ. Pollut.* **2024**, *360*, 124632. [CrossRef] [PubMed]
34. Sipps, K.; Patil, S.; Ochoa, L.; Chan, J.; Auguste, C.; Arbuckle-Keil, G.; Fahrenfeld, N.L. Quantitative and qualitative impacts of nitric acid digestion on microplastic identification via FTIR and Raman spectroscopy, implications for environmental samples. *Anal. Bioanal. Chem.* **2023**, *415*, 6809–6823. [CrossRef] [PubMed]
35. Wang, T.; Li, N.; Huang, X.; Li, H.; Gao, X.; Lu, K.; Du, W.; Zeng, Y. Integrated analysis of microplastics in human gallbladder and bile using multimodal detection techniques. *J. Hazard. Mater.* **2025**, *498*, 139897. [CrossRef] [PubMed]
36. Sun, J.; Sui, M.; Wang, T.; Teng, X.; Sun, J.; Chen, E.M. Detection and quantification of various microplastics in human endometrium based on laser direct infrared spectroscopy. *Sci. Total Environ.* **2024**, *906*, 167760. [CrossRef] [PubMed]
37. Wang, M.; Liu, Q.; Zhang, X.; Jiang, H.; Zhang, E.X. Identification and analysis of microplastics in human penile cancer tissues. *Sci. Total Environ.* **2025**, *969*, 178815. [CrossRef] [PubMed]
38. Zhang, K.; Yu, S.; Chen, S.; Zhou, Z.; Zhan, Y.; Zhang, E.X. Multimodal detection and analysis of microplastics in human clear cell renal cell carcinoma. *Environ. Pollut.* **2025**, *383*, 126729. [CrossRef] [PubMed]
39. Liu, S.; Wang, C.; Yang, Y.; Du, Z.; Li, L.; Zhang, M.; Ni, S.; Yue, Z.; Yang, K.; Wang, Y.; et al. Microplastics in three types of human arteries detected by pyrolysis-gas chromatography/mass spectrometry (Py-GC/MS). *J. Hazard. Mater.* **2024**, *469*, 133855. [CrossRef] [PubMed]
40. Pfeiffer En, F.; Fischer, E.K. Various Digestion Protocols Within Microplastic Sample Processing—Evaluating the Resistance of Different Synthetic Polymers and the Efficiency of Biogenic Organic Matter Destruction. *Front. Environ. Sci.* **2020**, *8*, 572424. [CrossRef]
41. Gulizia, A.M.; Brodie, E.; Daumuller, R.; Bloom, S.B.; Corbett, T.; Santana, M.M.F.; Motti, C.A.; Vamvounis, G. Evaluating the Effect of Chemical Digestion Treatments on Polystyrene Microplastics: Recommended Updates to Chemical Digestion Protocols. *Macromol. Chem. Phys.* **2022**, *223*, 2100485. [CrossRef]
42. Prata, J.C.; da Costa, J.P.; Duarte, A.C.; Rocha-Santos, E.T. Methods for sampling and detection of microplastics in water and sediment: A critical review. *TrAC Trends Anal. Chem.* **2019**, *110*, 150–159. [CrossRef]
43. Leonard, S.V.L.; Liddle, C.R.; Atherall, C.A.; Chapman, E.; Watkins, M.; Calaminus, S.D.J.; Rotchell, J.M. Microplastics in human blood: Polymer types, concentrations and characterisation using μFTIR. *Environ. Int.* **2024**, *188*, 108751. [CrossRef] [PubMed]
44. Guo, Y.; Rong, M.; Fan, Y.; Teng, X.; Jin, L.; Zhao, E.Y. The Presence of Microplastics in Human Semen and Their Associations with Semen Quality. *Toxics* **2025**, *13*, 566. [CrossRef] [PubMed]
45. Zhong, Y.; Yang, Y.; Zhang, L.; Ma, D.; Wen, K.; Cai, J.; Cai, Z.; Wang, C.; Chai, X.; Zhong, J.; et al. Revealing new insights: Two-center evidence of microplastics in human vitreous humor and their implications for ocular health. *Sci. Total Environ.* **2024**, *921*, 171109. [CrossRef] [PubMed]
46. Song, Y.; Zhang, J.; Shen, X.; Yang, L.; Jia, Y.; Song, F.; Huang, Y.; Han, B.; Zhou, S.; Zhang, N.; et al. Microplastics in stools and their influencing factors among young adults from three cities in China: A multicenter cross-sectional study. *Environ. Pollut.* **2025**, *364*, 125168. [CrossRef] [PubMed]
47. Özsoy, S.; Gündogdu, S.; Sezigen, S.; Tasalp, E.; Ikiz, D.A.; Kideys, E.A.E. Presence of microplastics in human stomachs. *Forensic Sci. Int.* **2024**, *364*, 112246. [CrossRef] [PubMed]
48. Zhang, J.; Wang, L.; Trasande, L.; Kannan, E.K. Occurrence of Polyethylene Terephthalate and Polycarbonate Microplastics in Infant and Adult Feces. *Environ. Sci. Technol. Lett.* **2021**, *8*, 989–994. [CrossRef]
49. Montano, L.; Raimondo, S.; Piscopo, M.; Ricciardi, M.; Guglielmino, A.; Chamayou, S.; Gentile, R.; Gentile, M.; Rapisarda, P.; Conti, G.O.; et al. First evidence of microplastics in human ovarian follicular fluid: An emerging threat to female fertility. *Ecotoxicol. Environ. Saf.* **2025**, *291*, 117868. [CrossRef] [PubMed]

50. Yang, Y.; Xie, E.; Du, Z.; Peng, Z.; Han, Z.; Li, L.; Zhao, R.; Qin, Y.; Xue, M.; Li, F.; et al. Detection of Various Microplastics in Patients Undergoing Cardiac Surgery. *Environ. Sci. Technol.* **2023**, *57*, 10911–10918. [CrossRef] [PubMed]
51. Massardo, S.; Verzola, D.; Alberti, S.; Caboni, C.; Santostefano, M.; Verrina, E.E.; Angeletti, A.; Lugani, F.; Ghiggeri, G.M.; Bruschi, M.; et al. MicroRaman spectroscopy detects the presence of microplastics in human urine and kidney tissue. *Environ. Int.* **2024**, *184*, 108444. [CrossRef] [PubMed]
52. Ren, F.; Pei, J.; Li, L.; Yuan, D.; Hao, F.; Qiao, P.; Liu, Y. The presence of microplastics in human semen and the protective role of nicotinamide mononucleotide against polystyrene nanoplastics-induced reproductive and early embryonic toxicity. *J. Hazard. Mater.* **2026**, *505*, 141557. [CrossRef] [PubMed]
53. Li, Z.; Zheng, Y.; Maimaiti, Z.; Fu, J.; Yang, F.; Li, Z.-Y.; Shi, Y.; Hao, L.-B.; Chen, J.-Y.; Xu, C. Identification and analysis of microplastics in human lower limb joints. *J. Hazard. Mater.* **2024**, *461*, 132640. [CrossRef] [PubMed]
54. Huang, S.; Huang, X.; Bi, R.; Guo, Q.; Yu, X.; Zeng, Q.; Huang, Z.; Liu, T.; Wu, H.; Chen, Y.; et al. Detection and Analysis of Microplastics in Human Sputum. *Environ. Sci. Technol.* **2022**, *56*, 2476–2486. [CrossRef] [PubMed]
55. Zhang, D.; Wu, C.; Liu, Y.; Li, W.; Li, S.; Peng, L.; Kang, L.; Ullah, S.; Gong, Z.; Li, Z.; et al. Microplastics are detected in human gallstones and have the ability to form large cholesterol-microplastic heteroaggregates. *J. Hazard. Mater.* **2024**, *467*, 133631. [CrossRef] [PubMed]
56. Halfar, J.; Čabanová, K.; Vávra, K.; Delongová, P.; Motyka, O.; Špaček, R.; Kukutschová, J.; Šimetka, O.; Heviánková, S. Microplastics and additives in patients with preterm birth: The first evidence of their presence in both human amniotic fluid and placenta. *Chemosphere* **2023**, *343*, 140301. [CrossRef] [PubMed]
57. Guo, X.; Wang, L.; Wang, X.; Li, D.; Wang, H.; Xu, H.; Liu, Y.; Kang, R.; Chen, Q.; Zheng, L.; et al. Discovery and analysis of microplastics in human bone marrow. *J. Hazard. Mater.* **2024**, *477*, 135266. [CrossRef] [PubMed]
58. Wang, J.; Kang, H.; Huang, X.; Liu, Y.; He, Y.; Jie, E.Y. Identification of microplastics in human tear fluid and meibum: Implications for dry eye disease pathogenesis. *J. Hazard. Mater.* **2025**, *489*, 137635. [CrossRef] [PubMed]
59. Zhang, L.; Tian, J.; Zhu, X.; Wang, L.; Yun, X.; Liang, L.; Duan, S. Cross-platform detection of microplastics in human biological tissues: Comparing spectroscopic and chromatographic approaches. *J. Hazard. Mater.* **2025**, *492*, 138133. [CrossRef] [PubMed]
60. Wu, D.; Feng, Y.; Wang, R.; Jiang, J.; Guan, Q.; Yang, X.; Wei, H.; Xia, Y.; Luo, Y. Pigment microparticles and microplastics found in human thrombi based on Raman spectral evidence. *J. Adv. Res.* **2023**, *49*, 141–150. [CrossRef] [PubMed]
61. Shim En, Y.; Min, H. Identification and Characterization of Microplastics in Human Cervicovaginal Lavage Fluids Using Raman Spectroscopy: A Preliminary Study. *Life* **2025**, *15*, 357. [CrossRef] [PubMed]
62. Wang, T.; Yi, Z.; Liu, X.; Cai, Y.; Huang, X.; Fang, J.; Shen, R.; Lu, W.; Xiao, Y.; Zhuang, W.; et al. Multimodal detection and analysis of microplastics in human thrombi from multiple anatomically distinct sites. *eBioMedicine* **2024**, *103*, 105118. [CrossRef] [PubMed]
63. Deng, C.; Zhu, J.; Fang, Z.; Yang, Y.; Zhao, Q.; Zhang, Z.; Jin, Z.; Jiang, H. Identification and analysis of microplastics in para-tumor and tumor of human prostate. *eBioMedicine* **2024**, *108*, 105360. [CrossRef] [PubMed]
64. Pironti, C.; Notarstefano, V.; Ricciardi, M.; Motta, O.; Giorgini, E.; Montano, E.L. First Evidence of Microplastics in Human Urine, a Preliminary Study of Intake in the Human Body. *Toxics* **2022**, *11*, 40. [CrossRef] [PubMed]
65. Umurhan, Y.; Songsart-Power, M.; Limbu, T.B.; Phan, E.T. Applications of Raman spectroscopy for microplastic detection and characterization: A comprehensive spectral reference. *Environ. Sci. Pollut. Res.* **2025**, *32*, 28630–28677. [CrossRef] [PubMed]
66. Araujo, C.F.; Nolasco, M.M.; Ribeiro, A.M.P.; Ribeiro-Claro, E.P.J.A. Identification of microplastics using Raman spectroscopy: Latest developments and future prospects. *Water Res.* **2018**, *142*, 426–440. [CrossRef] [PubMed]
67. Dai, H.; Li, H.; Qiu, W.; Deng, S.; Han, J.; Aminabhavi, E.T. Nondestructive analysis of plastic debris from micro to nano sizes: A state-of-the-art review on Raman spectroscopy-based techniques. *TrAC Trends Anal. Chem.* **2024**, *176*, 117750. [CrossRef]
68. Nava, V.; Frezzotti, M.L.; Leoni, E.B. Raman Spectroscopy for the Analysis of Microplastics in Aquatic Systems. *Appl. Spectrosc.* **2021**, *75*, 1341–1357. [CrossRef] [PubMed]
69. Al-Amin, K.; Kawsar, M.; Mamun, M.T.R.B.; Sahadat Hossain, E.M. Fourier transform infrared spectroscopic technique for analysis of inorganic materials: A review. *Nanoscale Adv.* **2025**, *7*, 6677–6702. [CrossRef] [PubMed]
70. Bhargava, R.; Wang, S.-Q.; Koenig, E.J.L. FTIR Microspectroscopy of Polymeric Systems. *Adv. Polym. Sci.* **2003**, *163*, 137–191. [CrossRef]
71. Käppler, A.; Fischer, D.; Oberbeckmann, S.; Schernewski, G.; Labrenz, M.; Eichhorn, K.-J.; Voit, B. Analysis of environmental microplastics by vibrational microspectroscopy: FTIR, Raman or both? *Anal. Bioanal. Chem.* **2016**, *408*, 8377–8391. [CrossRef] [PubMed]
72. Rotchell, J.M.; Austin, C.; Chapman, E.; Atherall, C.A.; Liddle, C.R.; Dunstan, T.S.; Blackburn, B.; Mead, A.; Filart, K.; Beeby, E.; et al. Microplastics in human urine: Characterisation using μFTIR and sampling challenges using healthy donors and endometriosis participants. *Ecotoxicol. Environ. Saf.* **2024**, *274*, 116208. [CrossRef] [PubMed]
73. Min, H.J.; Kim, K.S.; Kim, H.; Gong, J.; Jeong, E.J. Identification and characterization of microplastics in human nasal samples. *Int. Forum Allergy Rhinol.* **2024**, *14*, 1943–1946. [CrossRef] [PubMed]

74. Park En, H.; Park, B. Review of Microplastic Distribution, Toxicity, Analysis Methods, and Removal Technologies. *Water* **2021**, *13*, 2736. [CrossRef]
75. Roberto de Bruin, C.; de Rijke, E.; van Wezel, A.P.; Astefanei, E.A. Methodologies to characterize, identify and quantify nano- and sub-micron sized plastics in relevant media for human exposure: A critical review. *Environ. Sci. Adv.* **2022**, *1*, 238–258. [CrossRef]
76. Xu, J.-L.; Thomas, K.V.; Luo, Z.; Gowen, E.A.A. FTIR and Raman imaging for microplastics analysis: State of the art, challenges and prospects. *TrAC Trends Anal. Chem.* **2019**, *119*, 115629. [CrossRef]
77. Cowger, W.; Steinmetz, Z.; Gray, A.; Munno, K.; Lynch, J.; Hapich, H.; Primpke, S.; De Frond, H.; Rochman, C.; Herodotou, O. Microplastic Spectral Classification Needs an Open Source Community: Open Specy to the Rescue! *Anal. Chem.* **2021**, *93*, 7543–7548. [CrossRef]
78. Kozloski, R.; Cowger, W.; Arienzo, E.M.M. Moving toward automated μFTIR spectra matching for microplastic identification: Addressing false identifications and improving accuracy. *Microplast. Nanoplast.* **2024**, *4*, 27. [CrossRef]
79. De Frond, H.; Rubinovitz, R.; Rochman, E.C.M. MATR-FTIR Spectral Libraries of Plastic Particles (FLOPP and FLOPP-e) for the Analysis of Microplastics. *Anal. Chem.* **2021**, *93*, 15878–15885. [CrossRef] [PubMed]
80. Agilent Technologies. 8700 LDIR Chemical Imaging System. Available online: https://www.agilent.com/en/product/molecular-spectroscopy/ldir-chemical-imaging-spectroscopy/ldir-chemical-imaging-system/ldir-chemical-imaging-system (accessed on 6 July 2026).
81. Penn State Institute of Energy and the Environment (or Agilent Technologies). Agilent 8700 Laser Direct Infrared (LDIR) Chemical Imaging System Video. 14 May 2026. Available online: https://www.selectscience.net/SelectScience-TV/Videos/agilent-8700-laser-direct-infrared-ldir-chemical-imaging-system-video/?videoID=5368&fbclid=IwAR2ZZ27D9qJ1NpGdZHJ3UIk_ogSFUVb-sRTaHkQbfmPNSalECip9aM68mJM (accessed on 7 July 2026).
82. Isaac Chandran, P.J.; Veerasingam, E.S. Laser Direct Infrared Spectroscopy: A cutting-edge approach to microplastic detection in environmental samples. *Talanta* **2025**, *284*, 127284. [CrossRef] [PubMed]
83. Pagliaccia, B.; Ascolese, M.; Vannini, E.; Carretti, E.; Lubello, C.; Gori, E.R. Methodologic insights aimed to set-up an innovative Laser Direct InfraRed (LDIR)-based method for the detection and characterization of microplastics in wastewaters. *Sci. Total Environ.* **2025**, *967*, 178817. [CrossRef] [PubMed]
84. Tian, X.; Beén, F.; Bäuerlein, E.P.S. Quantum cascade laser imaging (LDIR) and machine learning for the identification of environmentally exposed microplastics and polymers. *Environ. Res.* **2022**, *212*, 113569. [CrossRef] [PubMed]
85. Tsuge, S.; Ohtani, H.; Watanabe, E.C. *Pyrolysis—GC/MS Data Book of Synthetic Polymers*; Elsevier: Amsterdam, The Netherlands, 2011.
86. Tan, Y.; Woodward, W.H.H.; Becker, D.; Luong, J.; Ellis-Hutchings, R.; Hart, K.; Kapur, M.B.; Meunier, D.M. Opportunities to improve polyethylene microparticle analysis by pyrolysis-gas chromatography/mass spectrometry. *Microplast. Nanoplast.* **2026**, *6*, 29. [CrossRef]
87. Zhang, K.; Yu, L.; Qu, L.; Hui, N.; Chen, L.; Wang, J.; Yan, H. Identifying and analyzing the microplastics in human aqueous humor by pyrolysis-gas chromatography/mass spectrometry. *iScience* **2025**, *28*, 112078. [CrossRef] [PubMed]
88. Zhou, Y.; Fu, B.; Che, J.; Ye, E.X. Simultaneous Determination of Six Common Microplastics by a Domestic Py-GC/MS. *Atmosphere* **2025**, *16*, 476. [CrossRef]
89. Li, Q.; Bai, Q.; Yu, S.; Liu, R.; Liu, E.J. Advances and challenges in the determination of micro- and nano-plastics by pyrolysis-gas chromatography-mass spectrometry. *TrAC Trends Anal. Chem.* **2025**, *189*, 118270. [CrossRef]
90. Seeley En, M.E.; Lynch, J.M. Previous successes and untapped potential of pyrolysis–GC/MS for the analysis of plastic pollution. *Anal. Bioanal. Chem.* **2023**, *415*, 2873–2890. [CrossRef] [PubMed]
91. Monikh, F.A.; Materić, D.; Valsami-Jones, E.; Grossart, H.-P.; Altmann, K.; Holzinger, R.; Lynch, I.; Stubenrauch, J.; Peijnenburg, W. Challenges in studying microplastics in human brain. *Nat. Med.* **2025**, *31*, 4034–4035. [CrossRef] [PubMed]
92. Kim, N.; Lee, J.H.; Lee, I.; Park, J.H.; Jung, G.S.; Lee, M.J.; Im, W.; Cho, S.; Choi, Y.S. Investigation of potential toxic effects of nano- and microplastics on human endometrial stromal cells. *Reprod. Toxicol.* **2025**, *132*, 108848. [CrossRef] [PubMed]
93. Ramsperger, A.F.; Bergamaschi, E.; Panizzolo, M.; Fenoglio, I.; Barbero, F.; Peters, R.; Undas, A.; Purker, S.; Giese, B.; Lalyer, C.R.; et al. Nano- and microplastics: A comprehensive review on their exposure routes, translocation, and fate in humans. *NanoImpact* **2023**, *29*, 100441. [CrossRef] [PubMed]
94. Zhu, L.; Xie, C.; Chen, L.; Dai, X.; Zhou, Y.; Pan, H.; Tian, K. Transport of microplastics in the body and interaction with biological barriers, and controlling of microplastics pollution. *Ecotoxicol. Environ. Saf.* **2023**, *255*, 114818. [CrossRef] [PubMed]
95. Pan, Y.; Janjua, T.I.; Thomas, K.V.; Shepherd, C.E.; Rauert, E.C. A critical review of micro- and nanoplastic permeation in the human body. *Microplast. Nanoplast.* **2026**, *6*, 21. [CrossRef]
96. Khan En, A.; Jia, Z. Recent insights into uptake, toxicity, and molecular targets of microplastics and nanoplastics relevant to human health impacts. *iScience* **2023**, *26*, 106061. [CrossRef] [PubMed]
97. Lai, H.; Liu, X.; Qu, E.M. Nanoplastics and Human Health: Hazard Identification and Biointerface. *Nanomaterials* **2022**, *12*, 1298. [CrossRef] [PubMed]

98. Mahmoudi, M.; Landry, M.P.; Moore, A.; Coreas, E.R. The protein corona from nanomedicine to environmental science. *Nat. Rev. Mater.* **2023**, *8*, 422–438. [CrossRef] [PubMed]
99. Yee, M.S.-L.; Hii, L.-W.; Looi, C.K.; Lim, W.-M.; Wong, S.-F.; Kok, Y.-Y.; Tan, B.-K.; Wong, C.-Y.; Leong, C.-O. Impact of Microplastics and Nanoplastics on Human Health. *Nanomaterials* **2021**, *11*, 496. [CrossRef] [PubMed]
100. Carvajal, B.; Sun, R.V.; Piderit, F.; Zazueta, A.; Tapia, C.V.; Gotteland, M.; Magne, F. Microplastics in Female Reproductive and Pregnancy Organs: A Systematic Review. *Life* **2026**, *16*, 746. [CrossRef] [PubMed]
101. Hunt, K.; Davies, A.; Fraser, A.; Burden, C.; Howell, A.; Buckley, K.; Harding, S.; Bakhbakhi, D. Exposure to microplastics and human reproductive outcomes: A systematic review. *BJOG An. Int. J. Obstet. Gynaecol.* **2024**, *131*, 675–683. [CrossRef] [PubMed]
102. Xue, J.; Xu, Z.; Hu, X.; Lu, Y.; Zhao, Y.; Zhang, E.H. Microplastics in maternal amniotic fluid and their associations with gestational age. *Sci. Total Environ.* **2024**, *920*, 171044. [CrossRef] [PubMed]
103. Xia, H.; Li, Y.; Wang, F.; Li, G.; Tan, Z.; Song, E.M. Human Exposure to Micro- and Nanoplastics: Trans-Barrier Transport, Tissue Accumulation, and Health Risks. *Environ. Health* **2026**, *ahead of print*. [CrossRef]
104. Nihart, A.J.; Garcia, M.A.; El Hayek, E.; Liu, R.; Olewine, M.; Kingston, J.D.; Castillo, E.F.; Gullapalli, R.R.; Howard, T.; Bleske, B.; et al. Bioaccumulation of microplastics in decedent human brains. *Nat. Med.* **2025**, *31*, 1114–1119. [CrossRef] [PubMed]
105. Monopoli, M.P.; Åberg, C.; Salvati, A.; Dawson, E.K.A. Biomolecular coronas provide the biological identity of nanosized materials. *Nat. Nanotechnol.* **2012**, *7*, 779–786. [CrossRef] [PubMed]
106. Breznica, P.; Koliqi, R.; Daka, E.A. A review of the current understanding of nanoparticles protein corona composition. *Med. Pharm. Rep.* **2020**, *93*, 342–350. [CrossRef] [PubMed]
107. Kopatz, V.; Wen, K.; Kovács, T.; Keimowitz, A.S.; Pichler, V.; Widder, J.; Vethaak, A.D.; Hollóczki, O.; Kenner, L. Micro- and Nanoplastics Breach the Blood–Brain Barrier (BBB): Biomolecular Corona's Role Revealed. *Nanomaterials* **2023**, *13*, 1404. [CrossRef] [PubMed]
108. Wolfram, J.; Yang, Y.; Shen, J.; Moten, A.; Chen, C.; Shen, H.; Ferrari, M.; Zhao, Y. The nano-plasma interface: Implications of the protein corona. *Colloids Surf. B Biointerfaces* **2014**, *124*, 17–24. [CrossRef] [PubMed]
109. Li, Y.; Liu, C.; Yang, H.; He, W.; Li, B.; Zhu, X.; Liu, S.; Jia, S.; Li, R.; Tang, K.H.D. Leaching of chemicals from microplastics: A review of chemical types, leaching mechanisms and influencing factors. *Sci. Total Environ.* **2024**, *906*, 167666. [CrossRef] [PubMed]
110. Pérez-Albaladejo, E.; Solé, M.; Porte, E.C. Plastics and plastic additives as inducers of oxidative stress. *Curr. Opin. Toxicol.* **2020**, *20–21*, 69–76. [CrossRef]
111. Kovacs, K.; Bodis, J.; Vass, E.R.A. Microplastics, Endocrine Disruptors, and Oxidative Stress: Mechanisms and Health Implications. *Int. J. Mol. Sci.* **2025**, *27*, 399. [CrossRef] [PubMed]
112. Yu, F.; Wu, J.; Wang, H.; Bao, Y.; Xing, H.; Ye, W.; Li, X.; Huang, M. Interaction of microplastics with perfluoroalkyl and polyfluoroalkyl substances in water: A review of the fate, mechanisms and toxicity. *Sci. Total Environ.* **2024**, *948*, 175000. [CrossRef] [PubMed]

Disclaimer/Publisher's Note: The statements, opinions and data contained in all publications are solely those of the individual author(s) and contributor(s) and not of MDPI and/or the editor(s). MDPI and/or the editor(s) disclaim responsibility for any injury to people or property resulting from any ideas, methods, instructions or products referred to in the content.